Exploring the link between micronutrients and phytoplankton in the Southern Ocean during the 2007 austral summer

Christel S. Hassler [1,2] *, Marie Sinoir [2,3], Lesley A. Clementson [2] and Edward C. V. Butler [2,4†]

[1] Plant Functional Biology and Climate Change Cluster, University of Technology Sydney, Broadway, NSW, Australia
[2] Marine and Atmospheric Research, Commonwealth Scientific and Industrial Research Organisation, Hobart, TAS, Australia
[3] University of Tasmania, Sandy Bay, TAS, Australia
[4] Ultramarine Concepts, Sandy Bay, TAS, Australia

*Correspondence:
Christel S. Hassler, Plant Functional Biology and Climate Change Cluster, University of Technology Sydney, PO Box 123, Broadway 2007, NSW, Australia.
e-mail: christel.hassler@uts.edu.au

†Present address:
Edward C. V. Butler, Australian Institute of Marine Science, Arafura Timor Research Facility, Darwin, NT, Australia.

Bottle assays and large-scale fertilization experiments have demonstrated that, in the Southern Ocean, iron often controls the biomass and the biodiversity of primary producers. To grow, phytoplankton need numerous other trace metals (micronutrients) required for the activity of key enzymes and other intracellular functions. However, little is known of the potential these other trace elements have to limit the growth of phytoplankton in the Southern Ocean. This study, investigates whether micronutrients other than iron (Zn, Co, Cu, Cd, Ni) need to be considered as parameters for controlling the phytoplankton growth from the Australian Subantarctic to the Polar Frontal Zones during the austral summer 2007. Analysis of nutrient disappearance ratios, suggested differential zones in phytoplankton growth control in the study region with a most intense phytoplankton growth limitation between 49 and 50°S. Comparison of micronutrient disappearance ratios, metal distribution, and biomarker pigments used to identify dominating phytoplankton groups, demonstrated that a complex interaction between Fe, Zn, and Co might exist in the study region. Although iron remains the pivotal micronutrient for phytoplankton growth and community structure, Zn and Co are also important for the nutrition and the growth of most of the dominating phytoplankton groups in the Subantarctic Zone region. Understanding of the parameters controlling phytoplankton is paramount, as it affects the functioning of the Southern Ocean, its marine resources and ultimately the global carbon cycle.

Keywords: subantarctic zone, pigments, Zn, Co, SAZ-Sense, trace element, subantarctic, polar

INTRODUCTION

The circumpolar Subantarctic Zone (SAZ) is an important biome of the global ocean which separates the High Nutrient Low Chlorophyll (HNLC) Southern Ocean from the mostly Low Nutrient Low Chlorophyll (LNLC) subtropical water from the Indian, Pacific, and Atlantic Oceans (Bowie et al., 2011a). The SAZ region forms a "belt" of important carbon sequestration accompanied by a phytoplankton biomass characterized by a low seasonality (Banse, 1996; Metzl et al., 1999; McNeil et al., 2001). However it is still unclear what parameters mostly constrain phytoplankton growth and how the dynamics of the SAZ region will be affected in the future.

The recent SAZ-Sense project took advantage of the natural variability in the SAZ region around Tasmania to study the impact of predicted future changes that will affect its functioning. This project focused on parameters likely to control phytoplankton biomass and carbon fixation, such as macro- (N, P, and Si) and micronutrients (essential trace metals), grazing and cell lysis promoted by the microbial loop, and as well, carbon export. Project outputs would help resolve the extent of future SAZ contribution to atmospheric CO_2 fixation and climate regulation. The SAZ region west of Tasmania (W-SAZ) is characteristic of most of the SAZ region nowadays (Trull et al., 2001), whereas the region east of Tasmania (E-SAZ), with greater intrusion of macronutrient-poor,

northern subtropical waters, and enhanced micronutrient inputs (e.g., iron, Hill et al., 2008; Bowie et al., 2009) mimics future predicted changes in the SAZ region. The two contrasting regions were compared to the waters south of Tasmania in the Polar Frontal Zone (PFZ) as an example of typical HNLC waters that could fuel the SAZ more significantly in the future (Herraiz Borreguero and Rintoul, 2011). The scientific rationale behind this study is summarized in Bowie et al. (2011a) and most of the results have been published in a special issue in Deep-Sea Research II (**Table A1 in Appendix**).

The difference in phytoplankton communities observed in the E-SAZ and the W-SAZ cannot be solely explained by considering macronutrients, light, grazing rates, and temperature (Kidston et al., 2011; Mongin et al., 2011; Pearce et al., 2011). It is believed that iron and silicic acid are mostly limiting the growth of phytoplankton, and thus, their ability to fix carbon (Bowie et al., 2009, 2011a; Lannuzel et al., 2011). Results from the SAZ-Sense project, demonstrate that silicic acid was limiting diatoms (de Salas et al., 2011; Fripiat et al., 2011) and iron was potentially limiting the growth of entire phytoplankton communities both in the W-SAZ and the PFZ (Lannuzel et al., 2011). Maximum photosynthetic quantum yield and results from iron phytoplankton uptake rates suggest that the W-SAZ was the main iron-limited region at the

time (Schoemann et al., unpublished). In the E-SAZ, iron was not limiting (Lannuzel et al., 2011) and diatoms were practically absent. Analysis of the phytoplankton communities revealed marked differences among the W-SAZ, PFZ, and E-SAZ, with the E-SAZ being dominated by nanoplankton (2–20 μm) and dinoflagellates (de Salas et al., 2011; Pearce et al., 2011). In the E-SAZ, despite possible light limitation (euphotic depth of 47 m and shallow mixed layer depth (MLD) of 16 m, but main mixed layer down to 79 m; Mongin et al., 2011; Westwood et al., 2011; **Table A1** in Appendix), the parameters controlling phytoplankton growth remain largely unresolved. Interestingly, phytoplankton carbon fixation and export were comparable or greater in the W-SAZ and the E-SAZ, despite a 1.4-fold average greater integrated chlorophyll *a* in the E-SAZ (Ebersbach et al., 2011; Jacquet et al., 2011; Westwood et al., 2011; **Table A1** in Appendix), demonstrating that iron limitation and carbon fixation and export were not directly related during SAZ-Sense. If the E-SAZ, represents the future of the SAZ region, then iron limitation is likely to be decreased and other micronutrients could play a role in capping phytoplankton growth, particularly if they are supplied by pathways differing from iron. It, thus, becomes urgent to explore the potential of other micronutrients to co-limit the growth of phytoplankton.

This study investigates the role of other micronutrients Zn, Co, Cu, which share several properties with iron in limiting the growth of phytoplankton, or at the least, in mediating community structure (Morel et al., 1994; Sunda and Huntsman, 1995a,b;

Buitenhuis et al., 2003; Saito and Goepfert, 2008; Saito et al., 2008). These micronutrients are co-factors of enzymes that catalyze essential reactions for the growth of phytoplankton, and key structural compounds (Morel and Price, 2003; Morel et al., 2003). Their possible limitation in marine systems are suggested by several laboratory studies (e.g., Morel et al., 1994; Saito et al., 2010) and phytoplankton have evolved high affinity uptake transport systems to survive under limited supply (Sunda and Huntsman, 1995b; Saito et al., 2002). These micronutrients are present at low concentrations in the open ocean (Lohan et al., 2002; Ellwood et al., 2005; Ellwood, 2008; Saito et al., 2010; Croot et al., 2011; Butler et al., in revision), they readily associate with organic compounds, and thus, are mostly complexed by organic ligands (Moffett and Brand, 1996; Saito and Moffett, 2001; Ellwood, 2004, 2008; Ellwood et al., 2005; Lohan et al., 2005), which decrease their bioavailability to sustain phytoplankton growth. This study also includes other potentially interesting micronutrients recently reported as essential in marine phytoplankton (Cd, Ni, e.g., Sunda and Huntsman, 2000; Lane et al., 2005; Dupont et al., 2008, 2010).

Because different phytoplankton species and functional groups have different biological requirements for growth (Buitenhuis et al., 2003; Sarthou et al., 2005; Sedwick et al., 2007; Saito and Goepfert, 2008) leading to differences in intracellular nutrient quota and drawdown (de Baar et al., 1997; Arrigo et al., 1999; Ho et al., 2003; Quigg et al., 2003, 2011; Twining et al., 2004a,b; Finkel et al., 2007, 2010), we investigate the relation between the
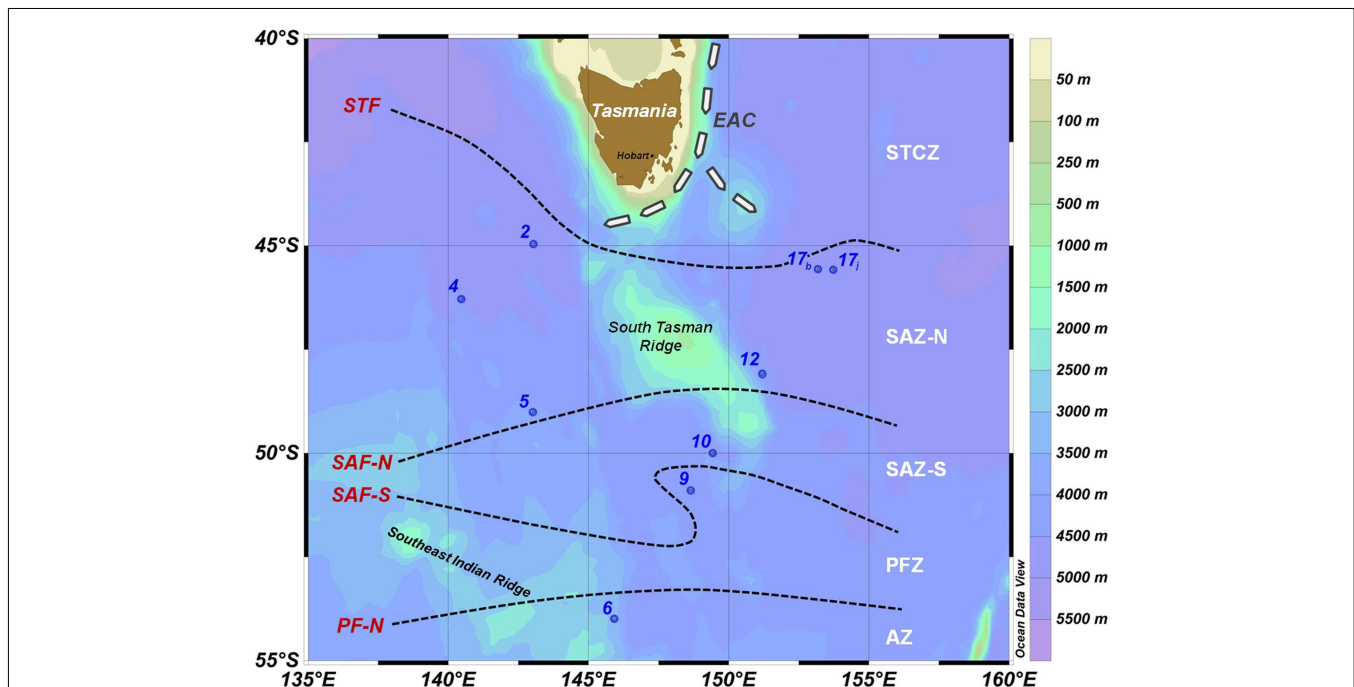

FIGURE 1 | Location of stations (number) as part of the SAZ – Sense voyage (January–February 2007) superimposed on bathymetry. The notations to the left of the dashed lines indicate the approximate location of fronts (following Sokolov and Rintoul, 2002) at the time of this voyage. The notations to the right define the zones between the fronts. The dashed arrows, tagged with EAC, indicate the East Australian Current extension characterized by mesoscale eddy features; the path around the south of Tasmania is the Tasman Outflow (Ridgway, 2007). Fronts (red text on left): STF, Subtropical Front; SAF-N, Subantarctic Front–North; SAF-S, Subantarctic Front–South; PF-N, Polar Front–North. Zones between fronts (white text on right): STCZ, Subtropical Convergence Zone; SAZ-N, Subantarctic Zone–North; SAZ-S, Subantarctic Zone–South; PFZ, Polar Frontal Zone; AZ, Antarctic Zone. Station 17 was sampled twice (on cast b and j on the 11 February 2007 and 17 February 2007, respectively).

distributions of dissolved nutrients and phytoplankton biomarker pigments, which can be used to infer phytoplankton community composition by using CHEMTAX at 5 locations during the SAZ-Sense expedition (e.g., de Salas et al., 2011). In addition, biological requirement for micronutrients is related to the size-aspect ratio (Sarthou et al., 2005; Hassler and Schoemann, 2009; Finkel et al., 2010). Size fractionation of pigments also pointed to different dominating phytoplankton groups in the SAZ and the Tasman Sea (de Salas et al., 2011; Hassler et al., 2011; Pearce et al., 2011). For these reasons, the link between micronutrients with large and small phytoplankton biomarker pigments is studied to gain further insight into their potential control on phytoplankton biomass, biodiversity, and contribution to carbon export. As done in previous studies, the disappearance ratio of nutrients is discussed to gain an understanding of the underlying processes at play (e.g., de Baar et al., 1997; Arrigo et al., 1999; Saito et al., 2010; Croot et al., 2011).

Table 1 | FI–SPE–ICP-MS conditions for determination of trace metals in seawater (O'Sullivan et al., in preparation).

Typical ICP-MS Conditions	
Nebuliser gas flow (mL/min)	1.02
Auxiliary gas flow (mL/min)	1.2
Plasma gas flow (mL/min)	15
ICP RF power (W)	1400
Skimmer/sample cones	Platinum
Sweep/readings	1
Readings/replicates	60
Number of replicates	1
Process signal profile	Sum
Dwell time (ms)	40
No of isotopes analyzed	21
Integration time (ms)	2400

MATERIALS AND METHODS
STUDY REGION

The SAZ-Sense voyage (*RV Aurora Australis*, 17 January–20 February 2007) visited contrasting water masses in the SAZ region around Tasmania (E-SAZ and W-SAZ) as well as further south in the PFZ, and crossed several fronts as summarized in **Figure 1**. The oceanography of the region is highly variable as a result of spatially heterogeneous inputs from subtropical waters from the north, and Subantarctic Mode Water and Antarctic Intermediate Water from the South (Bowie et al., 2011a; Herraiz Borreguero and Rintoul, 2011); nutrients from dust deposition and the continental margin (e.g., Bowie et al., 2009) provide a further overlay. The whole system creates naturally contrasting regions relevant to the study of controls on phytoplankton dynamics and their associated carbon fixation, recycling, and export. Oceanography of the region is summarized and put in a larger context elsewhere (Bowie et al., 2011b; Herraiz Borreguero and Rintoul, 2011). Critical properties of selected stations are summarized in **Table A1** in Appendix.

The SAZ-Sense project took advantage of the natural variability in the SAZ region around Tasmania to study the impact of predicted changes in major currents (e.g., Antarctic Circumpolar Current (ACC), East Australian Current (EAC, Hill et al., 2008; Toggweiler and Russell, 2008) that modulate important parameters for phytoplankton growth, such as the depth of the mixed layer, and micro- and macronutrient input (Bowie et al., 2009). The SAZ region west of Tasmania (W-SAZ) has low phytoplankton biomass characteristic of much of the SAZ region as it is nowadays (Trull et al., 2001), whereas the region East of Tasmania (E-SAZ) is characterized by high biomass persisting from the spring to summer, likely due to micronutrient (iron) input from eddy fields, arising from EAC activity and from Australian dust (Bowie et al., 2009, 2011a; Lannuzel et al., 2011; Mongin et al., 2011). In the future, the EAC is expected to strengthen (Hill et al., 2008) possibly bringing more eddies into the E-SAZ and Australian continent will become drier, with more terrigenous input from dust storms and bushfires expected to deposit in the South Tasman Sea (Matear et al., submitted).

Table 2 | Figures of Merit for FI–SPE–ICP-MS analyses.

	Detection limit [a] and precision [b]	SAFe S	SAFe D2	NASS 5
^{59}Co	0.003	0.006 ± 0.002	0.032 ± 0.003	0.188 ± 0.012
	8%	(0.005 ± 0.002)	(0.045 ± 0.004)	(0.187 ± 0.05)
^{60}Ni	0.03	2.47 ± 0.19	8.84 ± 0.51	4.52 ± 0.31
	6%	(2.31 ± 0.10)	(8.58 ± 0.30)	(4.31 ± 0.48)
^{65}Cu	0.05	0.56 ± 0.07	2.26 ± 0.11	4.82 ± 0.25
	5%	(0.51 ± 0.05)	(2.25 ± 0.11)	(4.67 ± 0.72)
^{66}Zn	0.22	<0.22	7.09 ± 0.49	1.42 ± 0.08
	7%	(0.064 ± 0.019)	(7.20 ± 0.50)	(1.56 ± 0.60)
^{111}Cd	0.005	<0.005	0.84 ± 0.02	0.178 ± 0.015
	3%	(0.001 ± 0.0002)	(0.986 ± 0.027)	(0.205 ± 0.030)

Average metal concentration (± 1 standard deviation) are given for SAFe S 430 and 125 ($n = 10$), SAFe D2 414 ($n = 8$), and NASS 5 ($n = 8$) reference samples. Consensus and certified values for these samples are given in bracket (http://www.es.ucsc.edu/~kbruland/GeotracesSaFe/kwbGeotracesSaFe.html, Consensus values from November 2011). Concentrations are given in nmol/kg. Note that here no UV-irradiation is done prior to analysis.

[a]*Detection limit calculated on $3 \times$ standard deviation of 0.1% HCl blank ($n = 8$).*

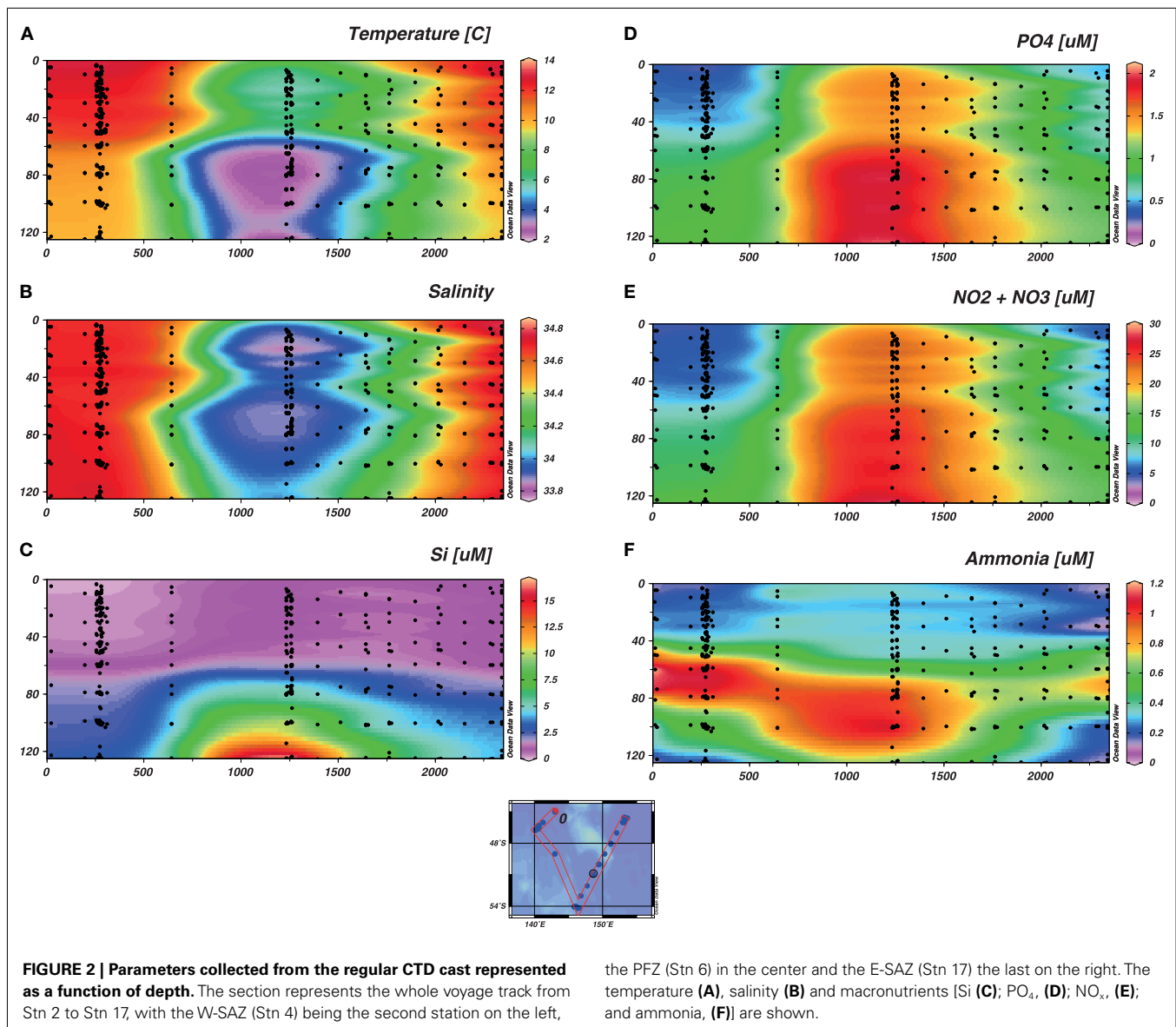[b]*Coefficient of variation of SAFe seawater D2 ($n = 8$).*

WATER SAMPLING

Samples for trace metal analyses and some pigment analyses (Stns 2, 6, 17, **Figure 1**) were taken using Teflon-coated Niskin X-1010 bottles (General Oceanics, USA) mounted on an autonomous rosette (Model 1018, General Oceanics, USA) and deployed using a Kevlar hydroline (Strongrope, AU). Water samples for micronutrient analysis were collected and filtered (Pall, Acropack 200) in a clean van under a HEPA filter (ISO Class 5 conditions). Sample acquisition and handling was as per GEOTRACES recommendations[1], using acid-washed non-contaminating material as detailed elsewhere (Bowie et al., 2009; Lannuzel et al., 2011). Samples were acidified using quartz-distilled HCl (1 mL L^{-1}, Seastar Baseline, Canada) and kept for 6 months doubly bagged in plastic boxes in clean storage, prior to analysis.

---

[1]www.geotraces.org/libraries/documents/Intercalibration/Cookbook.pdf

Salinity, temperature, fluorescence, and oxygen were obtained from calibrated conductivity-temperature-depth (CTD, SeaBird SBE9plus) data using water collected from Niskin bottles (General Oceanics) per Rosenberg (2007). Macronutrients (reactive phosphorus, PO_4; silicic acid, Si; nitrate-plus-nitrite, NO_x; ammonium, NH_4) were obtained by the analysis of unfiltered water using automated flow-injection analyzer and colorimetric techniques (Watson et al., 2005; Rosenberg, 2007). Samples were also collected for pigment determination (Stns 4, 9, 12). CTD deployments were performed close (within 0.1° latitude and longitude and 3.2 h) to the autonomous rosette to ensure that profiles of trace elements and other parameters describe the same water column (Bowie et al., 2011a).

MICRONUTRIENTS

Micronutrients were determined in an ISO class 5 Clean laboratory using automated flow-injection, solid phase extraction coupled to

FIGURE 2 | Parameters collected from the regular CTD cast represented as a function of depth. The section represents the whole voyage track from Stn 2 to Stn 17, with the W-SAZ (Stn 4) being the second station on the left, the PFZ (Stn 6) in the center and the E-SAZ (Stn 17) the last on the right. The temperature **(A)**, salinity **(B)** and macronutrients [Si **(C)**; PO_4, **(D)**; NO_x, **(E)**; and ammonia, **(F)**] are shown.

inductively coupled plasma-mass spectrometry (FI-SPE-ICP-MS; method and performance described in Butler et al., in revision, and full details in O'Sullivan et al. in preparation; **Table 1**). Briefly, 7.0-mL subsamples are decanted into acid-cleaned, 10-mL screw-cap polypropylene tubes, which are set in the tray of a CETAC ASX-520 auto sampler. Initiation of the ICP-MS control program sees the preconcentration/matrix-elimination step proceed on a PerkinElmer FIAS 400 system, with the sample stream merged with cleaned 1 M ammonium acetate buffer. The buffered sample (pH 5.7 ± 0.2) is then passed through the iminodiacetate (IDA) chelating sorbent (Toyopearl AF chelate-650M resin, 40–90 μm, Tosoh Bioscience GmbH, Germany) packed in 1-cm Global FIA (USA) cartridge mounted in the switching valve position. After loading, the solid phase is rinsed with buffered Milli-Q (Millipore, USA) deionized water to flush. With the switching valve moved to "Inject," the eluent [0.8 M HNO₃ (Seastar, Canada) +internal standard 10 ppb Rh] carries the adsorbed trace metals directly into the nebuliser (concentric quartz Meinhard-type with cyclonic spray chamber) and then into the quadrupole ICP-MS (PerkinElmer Elan DRC II, USA). The instrumental conditions for ICP-MS operation are summarized in **Table 1**. With each analysis of two casts (24 samples), calibration standards (standard additions to seawater sample for matrix matching), blanks and reference sea-waters (NASS 5, SAFe S, and D2) were run. The instrument was controlled, and data collected and put through primary processing, using Elan v3.4 software, with subsequent data processing done with MS Excel. "Figures of Merit" for this analytical method are presented in **Table 2**. Based on accuracy, blank, and performance in the measurement of reference seawaters (NASS 5, SAFe S, and D2), this version of the technique can be used for the measurement of Zn, Co, Cd, Cu, Ni, and Pb in seawater.

Seawater samples were not UV irradiated before analysis. Very recent work indicates that not all dissolved species of Co, and possibly Cu, in seawater will be measured under such circumstances, because some strongly complexed forms of these two metals only become detectable after photo-oxidative destruction of the organic ligands (Shelley et al., 2010; Biller and Bruland, 2012). Our method detects dissolved *labile* concentrations of metals; those which can be displaced by the IDA chelating sorbent. For the other metals Cd, Ni, Zn, and Pb, dissolved labile concentrations are comparable to total dissolved concentrations in oceanic waters. For our purposes, dissolved labile concentrations determined directly by the FI-SPE-ICP-MS method are a useful representation of the bioavailable fraction.

FIGURE 3 | Concentration of trace elements as a function of depth. The section represents the whole voyage track from Stn 2 to Stn 17, with the W-SAZ (Stn 4) being the second station on the left, the PFZ (Stn 6) in the center and the E-SAZ (Stn 17) the last on the right. The micronutrients Co **(A)**, Cu **(B)**, Zn **(C)**, Ni **(D)**, and Cd **(E)** are shown.
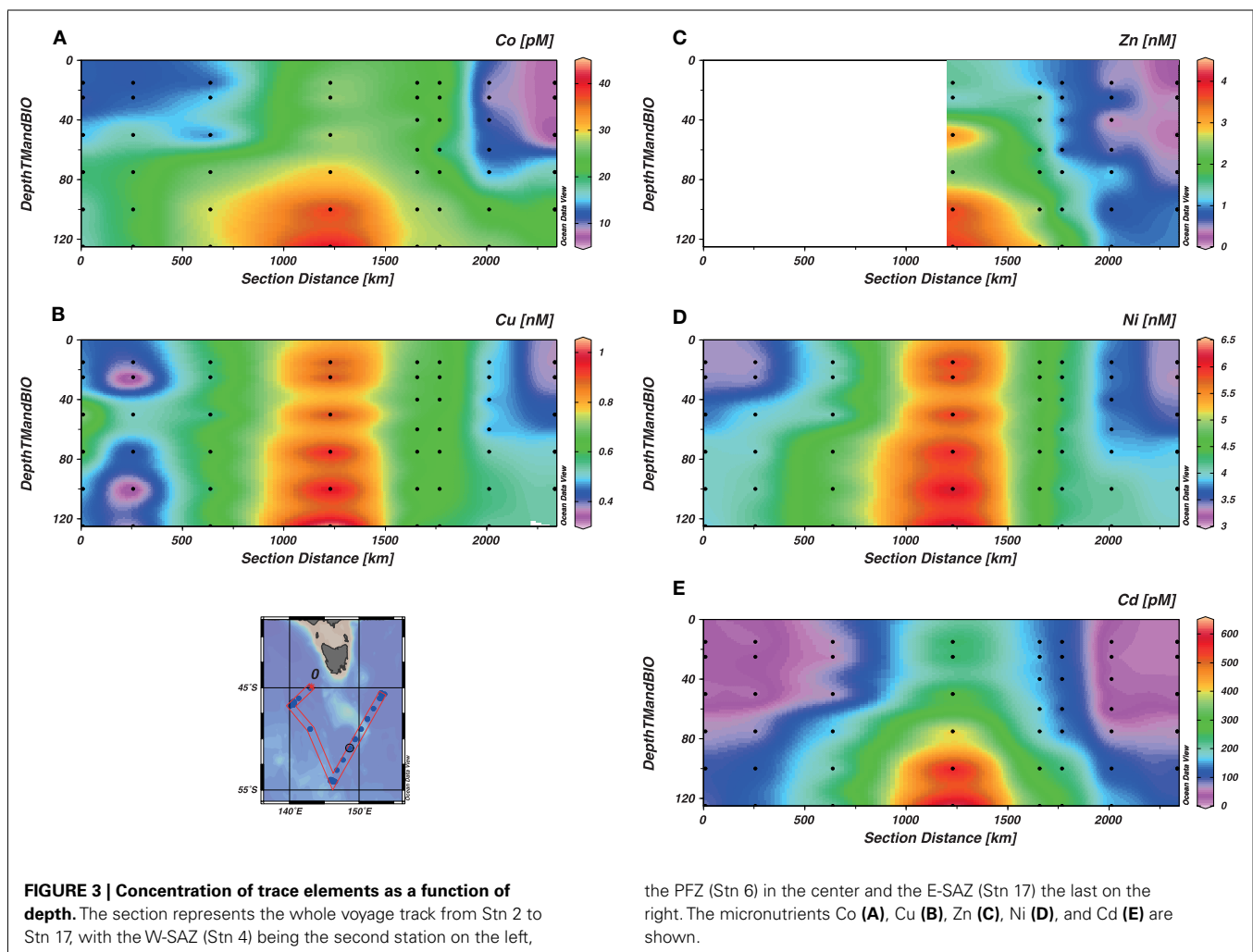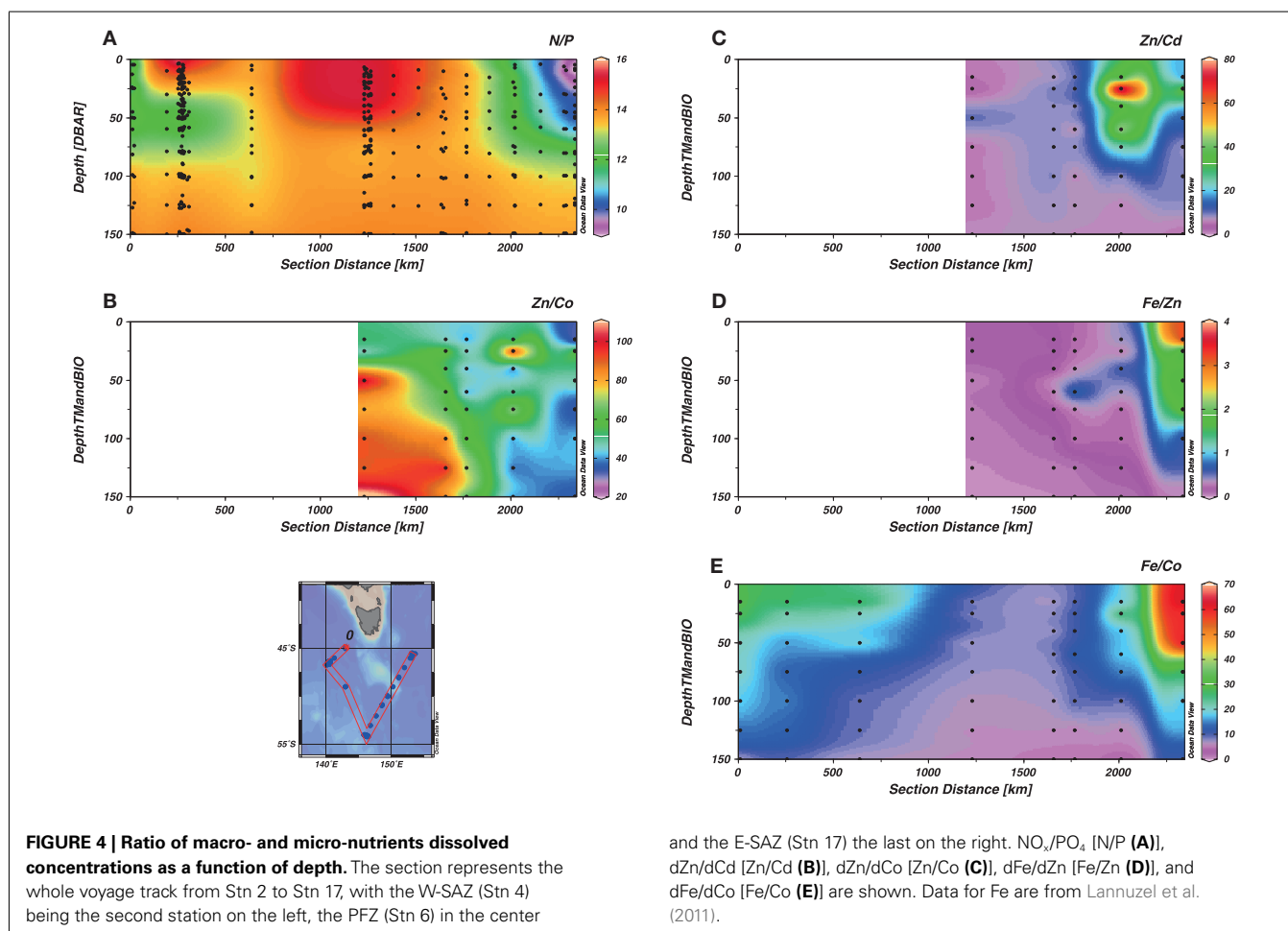
PIGMENT ANALYSIS

Pigment samples were collected in two size fractions, [$\geq 10\,\mu m$ (L-phyto) and $0.8-10\,\mu m$ (S-phyto)] using gentle sequential filtration (<5 mmHg) of approximately 1 L of seawater through 10 and $0.8\text{-}\mu m$ polycarbonate filters (Millipore). Filters were then stored in cryo-vials in liquid nitrogen prior to being analyzed back on shore. To extract the pigments, the filters were cut into small pieces and covered with 100% methanol (3 mL) in a 10-mL centrifuge tube. The samples were vortexed for about 30 s and then sonicated in an ice-water bath for 15 min in the dark. The samples were then kept in the dark at 4°C for approximately 15 h. After this time, $200\,\mu L$ water was added to the methanol such that the extract mixture was 90:10 methanol:water (vol:vol) and sonicated once more in an ice-water bath for 15 min. The extracts were quantitatively transferred to a clean a centrifuge tube and centrifuged to remove the filter paper. The final extract was filtered through a $0.2\text{-}\mu m$ membrane filter (Whatman, Anatop) prior to analysis by HPLC using a Waters – Alliance high performance liquid chromatography system, comprising a 2695XE separations module with column heater and refrigerated auto sampler and a 2996 photo-diode array detector. Immediately prior to injection the sample extract was mixed with a buffer solution (90:10 28 mM tetrabutyl ammonium acetate, pH 6.5: methanol) within the sample loop. After injection pigments were separated using a Zorbax

Eclipse XDB-C8 stainless steel 150 mm × 4.6 mm ID column with $3.5\,\mu m$ particle size (Agilent Technologies) and a binary gradient system with an elevated column temperature following a modified version of the van Heukelem and Thomas (2001) method. The separated pigments were detected at 436 nm and identified against standard spectra using Waters Empower software. Concentrations of chlorophyll a (Chl$a$), chlorophyll b (Chl$b$), and β,β-carotene in sample chromatograms were determined from standards (Sigma), while all other pigment concentrations were determined from standards (DHI, Denmark).

Pigments which relate specifically to an algal class are termed marker or diagnostic pigments (Jeffrey and Vesk, 1997; Jeffrey and Wright, 2006). Some of these diagnostic pigments are found exclusively in one algal class (e.g., alloxanthin in cryptophytes), while others are the principal pigments of one class, but are also found in other classes (e.g., fucoxanthin in diatoms and some haptophytes; 19′-butanoyloxyfucoxanthin in chrysophytes and some haptophytes). The presence or absence of these diagnostic pigments can provide a simple guide to the composition of a microalgal community, including identifying classes of small flagellates that cannot be determined by light microscopy techniques. Given that our dataset is limited, it was validated by comparison to the extensive total Chl$a$ measurements made by de Salas et al. (2011) and relative fluorescence recorded from the CTD. To push the comparison

FIGURE 4 | Ratio of macro- and micro-nutrients dissolved concentrations as a function of depth. The section represents the whole voyage track from Stn 2 to Stn 17, with the W-SAZ (Stn 4) being the second station on the left, the PFZ (Stn 6) in the center and the E-SAZ (Stn 17) the last on the right. NO_x/PO_4 [N/P **(A)**], dZn/dCd [Zn/Cd **(B)**], dZn/dCo [Zn/Co **(C)**], dFe/dZn [Fe/Zn **(D)**], and dFe/dCo [Fe/Co **(E)**] are shown. Data for Fe are from Lannuzel et al. (2011).

further, the CHEMTAX matrix used in de Salas et al. (2011) was applied to our data from stations 2, 6, and 17 to represent dominating large and small phytoplankton groups in the W-SAZ, PFZ, and E-SAZ, respectively.

DATA ANALYSES AND PLOTS

Sections of the voyage track (**Figure 1**) were plotted using Ocean Data View (version 4.5; Schlitzer, 2012). Since our goal is to compare micronutrients' distribution with phytoplankton biomass, size class, and functional groups, data above 125 m depth are presented. Full depth profiles and oceanography of trace elements have been discussed elsewhere (Lannuzel et al., 2011; Butler et al., in revision). The disappearance ratio between micronutrients with macronutrients (e.g., dCo/dPO$_4$, Arrigo et al., 1999, also referred to the dissolved ecological stoichiometric ratio, Saito et al., 2010) was

used as a proxy for phytoplankton uptake and growth rate (Arrigo et al., 1999; Cullen et al., 2003; Finkel et al., 2010; Croot et al., 2011). To identify the potential of each micronutrient to limit the growth of phytoplankton, the disappearance ratio is compared to phytoplankton cellular quotas, reflecting their biological requirement for growth, and dissolved macronutrient (e.g., NO$_x$/PO$_4$) and micronutrient (e.g., dZn/dCd) spot ratios, reflecting maximal micronutrient stock available for phytoplankton growth. It is to be noted that chemical speciation is not considered in this study. The labile dissolved metal considered likely overestimates the fraction that is bioavailable to support phytoplankton growth.

The statistical relations between micro- and macronutrient with temperature, salinity, chlorophyll *a*, and biomarker pigments were analyzed using the Excel package XLSTAT. Depths of the

Table 3 | Summary of dissolved disappearance ratios and biological requirement for phytoplankton growth for Cd, Zn, Co, Ni, and Cu.
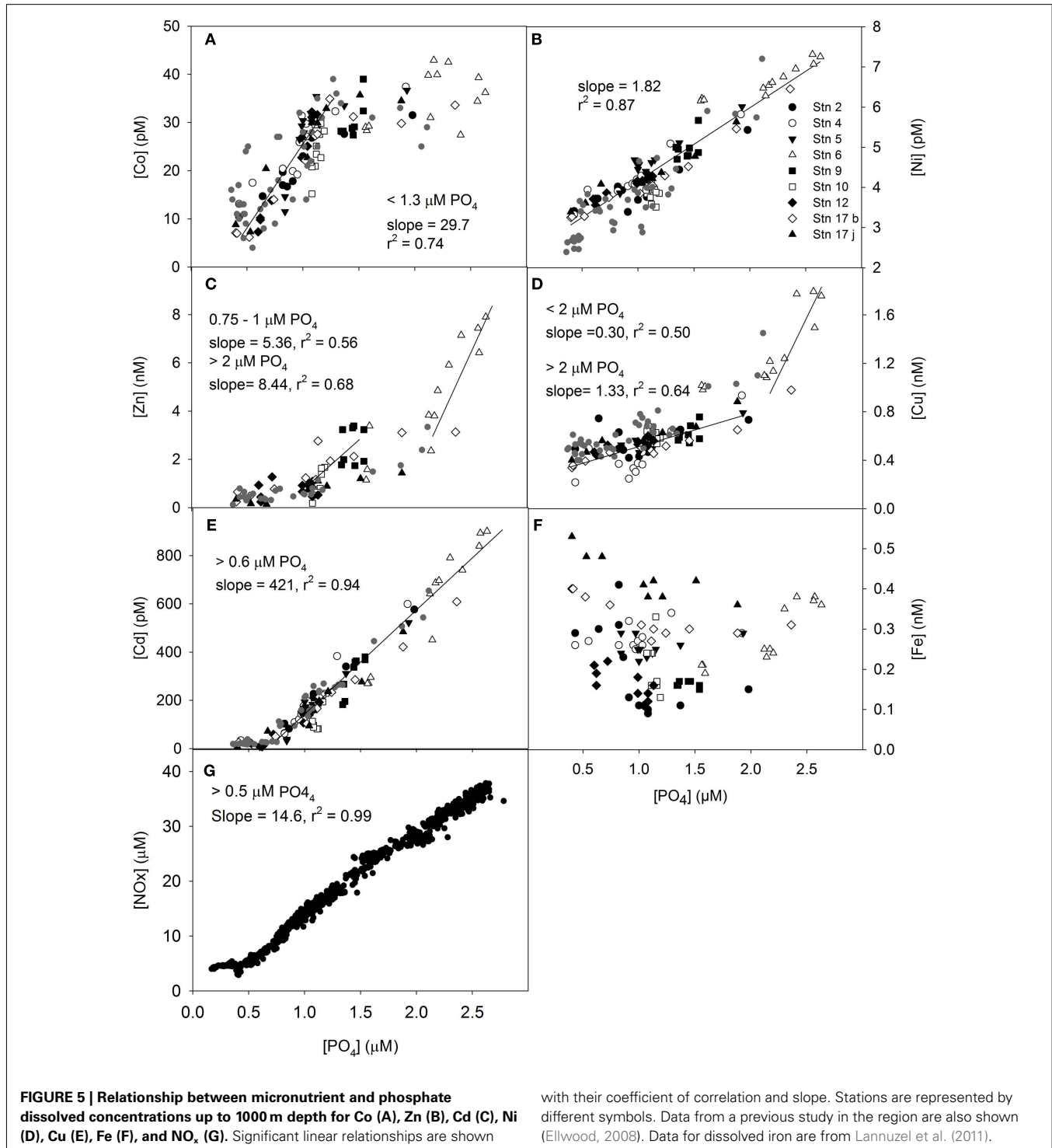
Micronutrient (M)	dM/PO$_4$	r^2	Depth (m)	Location
DISSOLVED DISAPPEARANCE RATIO (dM/PO$_4$, μmol mol^{-1})				
Cd	323	0.88	15–100	Southern Ocean (SAZ and PFZ, >0.6 μM PO$_4$)[a]
	461	0.94	30–100	Southern Ocean (SAZ and PFZ, >0.6 μM PO$_4$)[b]
	608	0.89	0–125	Southern Ocean (Ross Sea)[c]
	450	0.87	20–150	Subarctic Pacific (<1.2 μM PO$_4$)[d,e]
Zn	1637	0.61	15–100	Southern Ocean (SAZ and PFZ, >0.6 μM PO$_4$)[a]
	NA	0.001	30–100	Southern Ocean (SAZ and PFZ)[b]
	484	0.79	0–125	Southern Ocean (Ross Sea)[c]
	4857	0.73	>500	Southern Ocean (Drake passage and Zero meridian)[f]
	~2000–7000		0–400	
	251–370	0.70–0.99	8–150	Subarctic Pacific (<1.2 μM PO$_4$)[d,g]
	797	0.99	30–300	Southern Ocean (Drake Passage)[g,h]
Co	17	0.79	15–100	Southern Ocean (SAZ and PFZ)[a]
	25	0.62	30–100	Southern Ocean (SAZ and PFZ)[b]
	19	0.54	0–125	Southern Ocean (Ross Sea)[c]
	35–40	0.98–0.99	8–150	Subarctic Pacific[d,g]
	38	0.87	5–500	Southern Ocean (Ross Sea)[h]
Ni	1881	0.84	15–100	Southern Ocean (SAZ and PFZ)[a]
	1903	0.72	30–100	Southern Ocean (SAZ and PFZ)[b]
	1181	0.61	0–125	Southern Ocean (Ross Sea)[c]
Cu	441	0.73	15–100	Southern Ocean (SAZ and PFZ)[a]
	598	0.80	30–100	Southern Ocean (SAZ and PFZ)[b]
	846	0.72	0–125	Southern Ocean (Ross Sea)[c]
	430–450	0.96–0.99	0–985	North Pacific[d,j,k]
	680	0.92	30–300	Southern Ocean (Drake Passage)[h,k]

Strain	Zn/P*[g]	Co/P**[g]	Cu/P[k]
BIOLOGICAL REQUIREMENT FOR PHYTOPLANKTON GROWTH (CELLULAR M/P, μmol mol^{-1})			
E. huxleyi	1272 (0.7μ_{max})	264 (0.9μ_{max})	35 (0.9μ_{max}, low Cu)
			758 (0.9μ_{max}, high Cu)
T. oceanica	63 (0.9μ_{max})	1314 (0.7μ_{max})	216 (0.9μ_{max})
T. pseudonana	232 (0.6μ_{max})	1675 (0.5μ_{max})	NA
Synechococcus sp	ND	8.5 (0.6μ_{max})	NA

[a]*This study*; [b]*Ellwood (2008)*; [c]*Fitzwater et al. (2000)*; [d]*Martin et al. (1989)*; [e]*Sunda and Huntsman (2000)*; [f]*Croot et al. (2011)*; [g]*Sunda and Huntsman (1995a)*; [h]*Martin et al. (1990)*; [i]*Saito et al. (2010)*; [j]*Bruland (1980)*; [k]*Sunda and Huntsman (1995b)*.

* No Co added. ** No Zn added. ND = not detected, NA = not applicable.

mixed layer and the euphotic zone (Westwood et al., 2011) were used to define the depths considered in statistical tests and comparison (0–100 m for stations 9, 0–75 m for other stations; **Table A1** in Appendix). This results in dataset of 32 observations for which measurements of physical parameters, micro- and macronutrients, as well as biological parameters, were considered. Correlation tests were done using Pearson's coefficient with a 95% interval of confidence to highlight the occurrence of significant positive or

negative linear relationship between two parameters. The most significant relationships are graphically presented. Canonical Correspondence Analysis (CCA) was done to extract the pattern and illustrate the relation existing between the different parameters and observations. CCA was applied to represent the correspondence between (i) biological and physical parameters with the chemistry of the sites, and (ii) small and large phytoplankton communities and micronutrients.

FIGURE 5 | Relationship between micronutrient and phosphate dissolved concentrations up to 1000 m depth for Co (A), Zn (B), Cd (C), Ni (D), Cu (E), Fe (F), and NOx (G). Significant linear relationships are shown with their coefficient of correlation and slope. Stations are represented by different symbols. Data from a previous study in the region are also shown (Ellwood, 2008). Data for dissolved iron are from Lannuzel et al. (2011).

RESULTS

WATER MASSES

A snapshot of the hydrology along the relevant portion of the SAZ-Sense voyage track is shown in **Figure 2**. Temperature and salinity (**Figures 2A,B**, respectively) broadly characterize the regional water masses (see also Bowie et al., 2011b, with front definitions after Sokolov and Rintoul, 2002). The bulk was SAZ with salinity and temperature in the respective ranges, 34.2–34.8 and 2–12°C. The northernmost stations, west and east, were very close to the Subtropical Front (STF) with salinities at 34.9 (and temperature at 150 falling from 12 to 10°C across the STF, data not shown). The Polar Front is classically delineated by the subsurface $T_{min} < 2$°C, that occurs deeper than the section shown. A less precise indicator is surface salinity falling below 34 for the southernmost station (**Figure 2B**). The oceanography of the region during the SAZ-Sense expedition is fully described in Bowie et al. (2011b).

MACRONUTRIENTS

Sections of Si, PO_4, NO_x, and NH_4 are depicted in **Figures 2C–F**, respectively. PO_4 and NO_x showed very similar progressions along the voyage track. In northern SAZ surface waters, PO_4 was drawn

down to ≤ 0.5 μM and NO_x to ≤ 5 μM. Beyond the SAF-S front, concentrations began to ramp up, with surface waters ~1.5 μM PO_4 and ~20 μM NO_x. The nutricline typically varied between 60 and 80 m throughout the study region. Si was strongly depleted to a few micromolar concentrations in the upper 60 m for all stations (**Figure 2C**). Only beneath the nutricline, and poleward of SAF-S into PFZ waters, did Si begin to increase in concentration. NH_4 ranged from undetectable (<0.01 μM) to <0.4 μM in surface waters (**Figure 2F**). It has distinct subsurface maxima at the nutricline and deeper (to 120 m) at all stations, but they are more pronounced (>1 μM) on the western side of the voyage track than the east. Beyond 200 m (data not shown), NH_4 declined rapidly to background levels (≤ 0.01 μM). NH_4 is a useful indicator of remineralization of organic matter. Data demonstrated a significant remineralization just below the MLD in the W-SAZ and in the PFZ but not in the E-SAZ (**Figure 2; Table A1** in Appendix).

MICRONUTRIENTS

Dissolved labile concentrations of micronutrient metals along the voyage track are shown in **Figure 3**. Complete records have been plotted for Cd, Co, Cu, and Ni, but stations before Stn 6 were
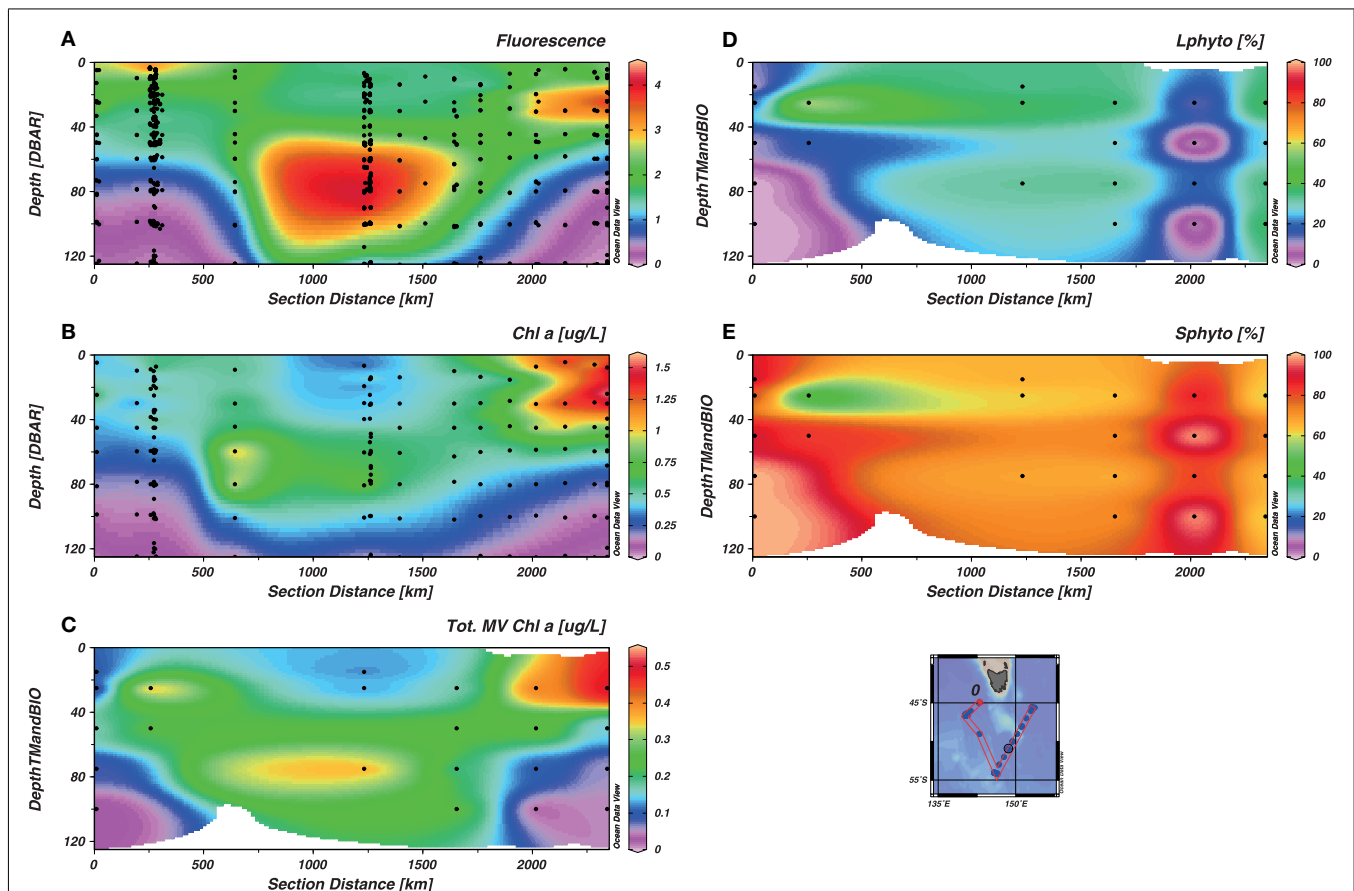

FIGURE 6 | Distribution of phytoplankton biomass as a function of depth. The section represents the whole voyage track from Stn 2 to Stn 17, with the W-SAZ (Stn 4) being the second station on the left, the PFZ (Stn 6) in the center and the E-SAZ (Stn 17) the last on the r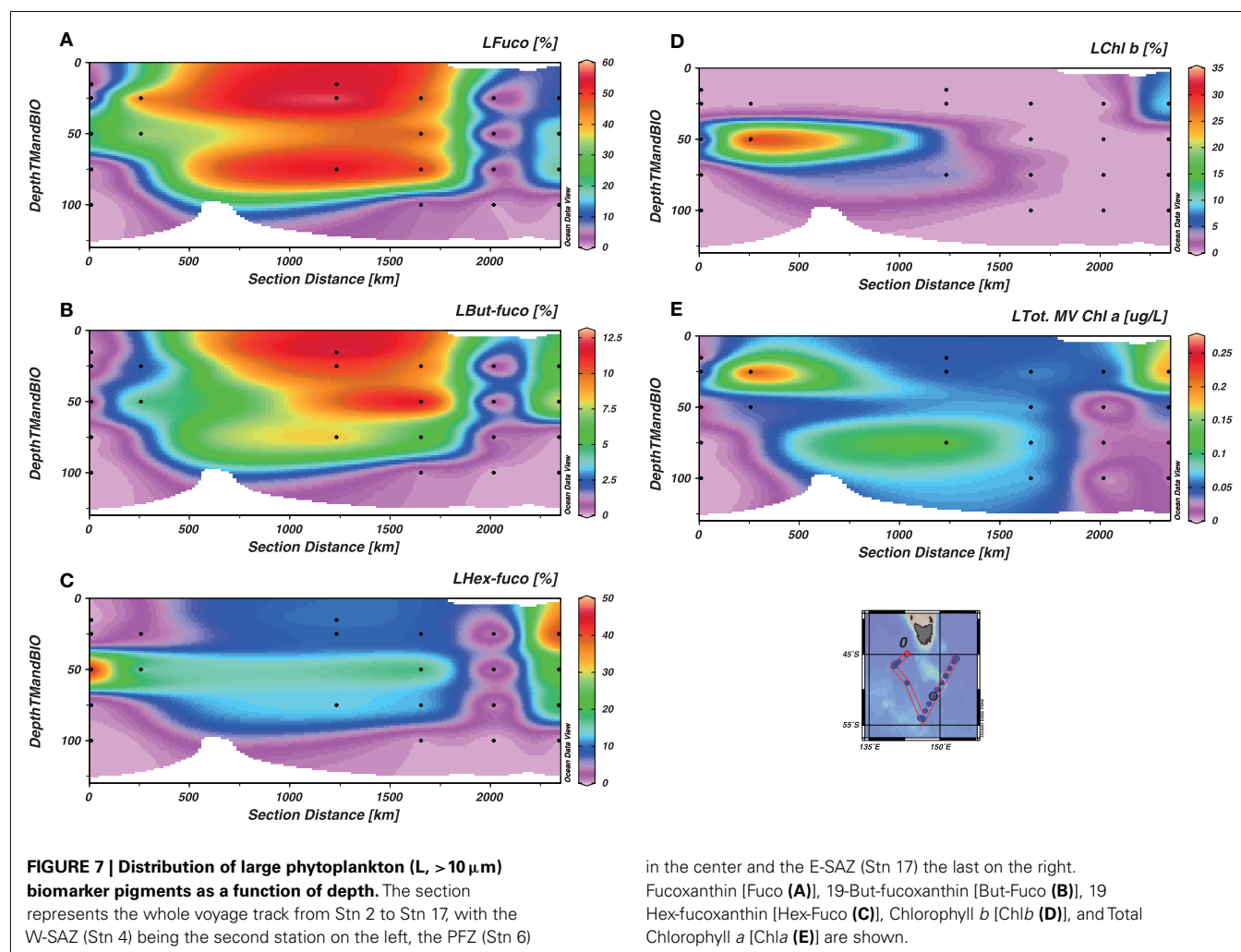ight. The fluorescence from the CTD [CTDFLUORO **(A)**], the total chlorophyll *a* (Chl*a*) measured by the team of Simon Wright [de Salas et al., 2011 **(B)**], the total Chl*a* data used in this study **(C)** are shown. In addition, the relative size distribution between large [L-phyto, >10 μm **(D)**] and small phytoplankton [S-phyto, 0.8–10 μm, **(E)**] are shown.

assessed as contaminated for Zn. The contaminated results were identified by irregularities in the depth profiles and recurrent outliers in property-property plots (i.e., metal vs. hydrological properties, metal vs. macronutrient (e.g., Si), and metal vs. metal). The distributions of these micronutrients in the SAZ-Sense study region is fully described in Butler et al., in revision. Cd, Cu, and Ni were closely related to PO_4 (**Figure 2D** and below), but the extent of their biological depletion was quite different. Relative to a reference depth of 150–200 m (see Bowie et al., 2011b), the depletion of Cd was 6 to >96%, that of Cu 11–35%, and Ni 7–20%. For each, the surface water depletion declined poleward. Co was also strongly depleted (31–70%). Zn was more comparable to the macronutrient Si in being depleted in most surface waters. Its depletion often extended well into the water column (≥ 200 m), so a reference depth of 150–200 m was not suitable for evaluating degree of depletion.

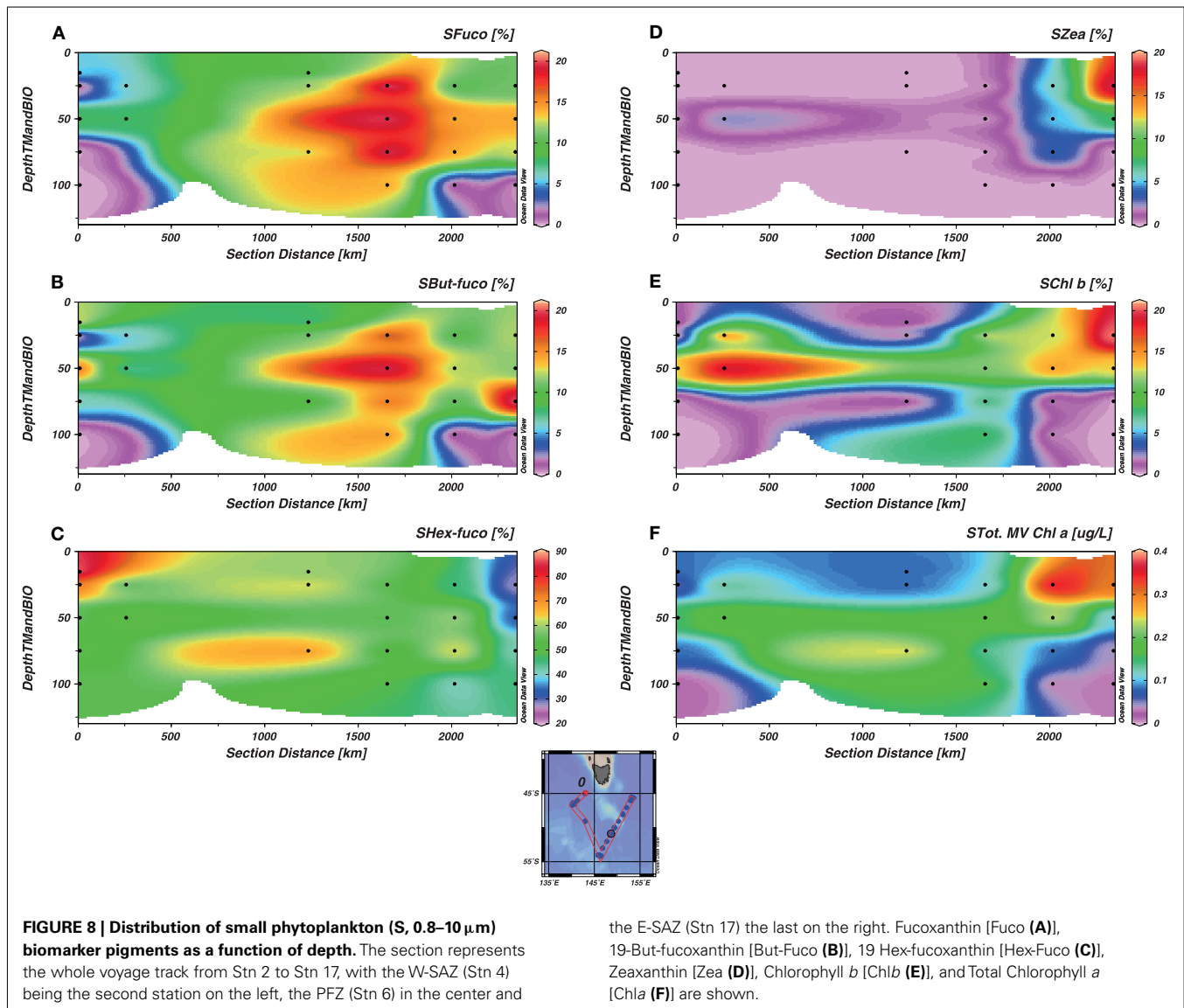### NUTRIENTS SPOT AND DISAPPEARANCE RATIO

Considering data from all depths, the macronutrient ratios between NO_x and PO_4 for the study region were close to an optimal value of 16 [14.6 ± 0.07 (standard error), $r^2 = 0.98$, $n > 750$, **Figure 5G**; Redfield et al., 1963]. However, a kink was observed

for $[PO_4] < 0.5\,\mu M$ (**Figure 5G**), suggesting that less NO_x was relatively consumed in surface water of the W-SAZ and E-SAZ. The dissolved NO_x/PO_4 spot ratios are suboptimal in the W-SAZ (at depth) and the E-SAZ regions (**Figure 4A**). Considering data from 0 to 100 m depth only (**Figure A1G** in Appendix), a close to optimal disappearance ratio was observed (slope 18.0 ± 0.18, $r^2 = 0.98$) for phosphate concentrations between 0.5 and 1.6 μM. For $[PO_4] > 1.6\,\mu M$, representing waters from the PFZ (Stn6), a significantly lower N/P disappearance ratio was observed (slope 7.00 ± 0.40, $r^2 = 0.85$). Because Fe, Zn, and Co could limit or co-limit the growth of oceanic phytoplankton (e.g., Martin et al., 1990; Morel et al., 1994; Coale et al., 2003), and Zn, Co, Cd are interchangeable enzymatic co-factors that can all support the growth of some marine phytoplankton (Price and Morel, 1990; Sunda and Huntsman, 1995b; Timmermans et al., 2001), the ratios between these micronutrients were investigated (**Figures 4B–E; Table A2** in Appendix). Dissolved zinc was present in excess compared to Co (dZn/dCo > 1, **Figure 4B**) with greatest ratios in the PFZ (Stn 6) and lowest ratios in the surface of the E-SAZ (Stn 17). The ratio dZn/dCd was close to unity in the PFZ and greater at Stn 12 just south of the E-SAZ. The ratios dFe/dZn and dFe/dCo (**Figures 4D,E**) were lower at the PFZ and greater in the

FIGURE 7 | Distribution of large phytoplankton (L, >10 μm) biomarker pigments as a function of depth. The section represents the whole voyage track from Stn 2 to Stn 17, with the W-SAZ (Stn 4) being the second station on the left, the PFZ (Stn 6) in the center and the E-SAZ (Stn 17) the last on the right. Fucoxanthin [Fuco **(A)**], 19-But-fucoxanthin [But-Fuco **(B)**], 19 Hex-fucoxanthin [Hex-Fuco **(C)**], Chlorophyll b [Chlb **(D)**], and Total Chlorophyll a [Chla **(E)**] are shown.

surface waters of the E-SAZ. For all micronutrients, except Fe, a disappearance ratio could be calculated from the linear regression between dissolved micronutrient and PO_4 concentrations (**Table 3**; **Figure 5**; **Figure A1** in Appendix). A kink was observed at low PO_4 concentrations (<0.5–$0.6\,\mu M\ PO_4$) for Cd and Zn and below $2\,\mu M\ PO_4$ for Cu. Ni is the only micronutrient for which no kink was observed. For Zn, data suggested two kinks separated by a plateau between 1.5 and $2\,\mu M\ PO_4$, however, the coefficient of correlation considering all data between 0 and $2\,\mu M\ PO_4$ was only slightly lower ($r^2 = 0.47$, slope $1764\,\mu mol\ Zn\ mol^{-1}\ PO_4$, **Figure 5B**). For Co, Zn, and Cu inter-station differences were observed (**Figure 5**). For Co, Stns 6, and 9 were on the plateau (**Figure 5A**) and the slope dCo/PO_4 was the greatest for Stns 5 and 10 (slope of 66–77 $\mu mol\ mol^{-1}$) as compared to the other stations (32–49). For Zn, no correlation ($r^2 < 0.5$) was observed for Stns 12 and 17, and greater dZn/PO_4 slopes (9–11 $\mu mol\ mol^{-1}$) were observed at Stns 9 and 10, suggesting greater Zn biological uptake at these stations. Correlations between Cu and PO_4

dissolved concentrations ($r^2 > 0.5$) were only observed at Stns 4 ($r^2 = 0.94$, slope $= 0.65$), 5 ($r^2 = 0.78$, slope $= 0.26$ mmol mol^{-1}), 12 ($r^2 = 0.83$, slope $= 0.24$ mmol mol^{-1}), and 17 ($r^2 = 0.94$ and 0.90, slope $= 0.19$ and 0.28 mmol mol^{-1}). When considering only the data from the top 100 m for all stations, the relation between micronutrients and PO_4 was slightly altered (**Table 3**; **Figure A1**, **Table A2** in Appendix). In this case, the disappearance ratios followed the order Ni $\sim$ Zn $>$ Cu $\sim$ Cd $>$ Co. The disappearance ratio for Zn was 5.1 and 96 times greater than for Cd and Co, respectively, suggesting greater biological utilization of Zn as compared to Cd and Co. Similar ratios were obtained using NO_x, whereas the significance of the correlation was much lower using Si (see **Figure A1** in Appendix). Considering the disappearance ratios calculated in surface water (0–100 m) and at depth (125–1000 m) for each station (**Table A1** in Appendix), revealed interesting trends. For all metals, except Co, the surface disappearance ratio in surface waters was equal or lower that the ratio calculated at depth. In addition, a loss of significant correlation between

FIGURE 8 | Distribution of small phytoplankton (S, 0.8–10 μm) biomarker pigments as a function of depth. The section represents the whole voyage track from Stn 2 to Stn 17, with the W-SAZ (Stn 4) being the second station on the left, the PFZ (Stn 6) in the center and the E-SAZ (Stn 17) the last on the right. Fucoxanthin [Fuco **(A)**], 19-But-fucoxanthin [But-Fuco **(B)**], 19 Hex-fucoxanthin [Hex-Fuco **(C)**], Zeaxanthin [Zea **(D)**], Chlorophyll b [Chl$b$ **(E)**], and Total Chlorophyll a [Chl$a$ **(F)**] are shown.

dissolved metal and phosphate was observed in the PFZ. Generally, a region between 49 and 50°S with greater disappearance ratios separated the surface waters between the SAZ and the PFZ (**Table A1** in Appendix).
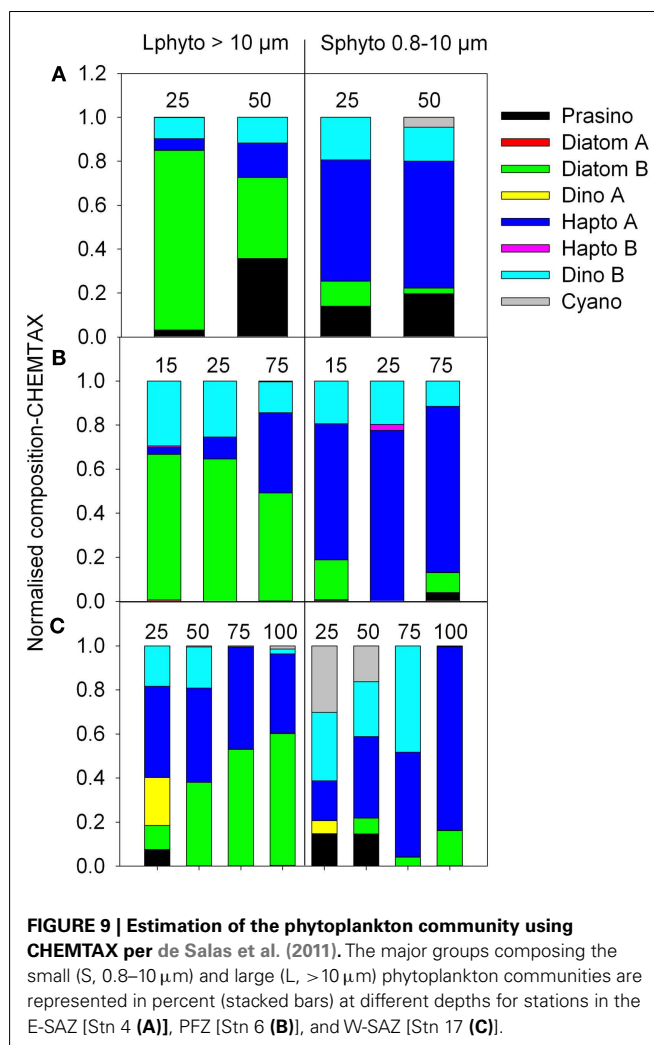
CHLOROPHYLL AND BIOMARKER PIGMENTS

Our dataset for total Chl*a* (**Figure 6C**) showed good correlation with the more extensive dataset from the fluorometer (CTD data, **Figure 6A**) and previous pigment analysis (de Salas et al., 2011, **Figure 6B**). The maximum Chl*a* concentration was observed in the surface of the E-SAZ (Stn 17) and the W-SAZ (Stn 4) and at depth in the PFZ (Stn 12). Total Chl*a* data from de Salas et al. (2011) were greater than our data, likely reflecting different extraction procedures and our sequential filtration step. Sequential filtration removes larger phytoplankton, decreasing clogging of the filter, and avoiding an overestimation of pigments' concentration.

In the study region, contrasting distribution of phytoplankton from different size classes was observed (**Figures 6D,E**). Small phytoplankton (0.8–10 µm, S-phyto) dominated at all stations, except in surface water of the W-SAZ (stn 4). In the northern W-SAZ waters (Stn 2) and south of the E-SAZ (Stn 12), S-phyto represented >80% of the total Chl*a*. Large phytoplankton (≥10 µm, L-phyto) represented a significant fraction (25–40%) of total Chl*a* only in the PFZ, Stn 9, and in the E-SAZ.

Using the distribution of the relative biomarker pigment concentrations (normalized against Chl*a*), dominating phytoplankton groups can be identified (Jeffrey and Wright, 2006). Maximum Chl*a* associated with larger phytoplankton correlated with total Chl*a* distribution (**Figures 6 and 7**). Large phytoplankton, present at the depth of Chl*a* maximum were mainly diatoms in the W-SAZ and PFZ (as indicated by a clear dominance of fucoxanthin) and were mainly haptophytes in the E-SAZ (dominance of 19-hexanoyloxyfucoxanthin, **Figure 7**). In the PFZ and E-SAZ, the Chl*a* associated with small phytoplankton correlated with total Chl*a* maximum (**Figures 6 and 8**). In the W-SAZ, most of the S-phyto were present at 50 m, below the total Chl*a* maximum (**Figure 8**). Haptophytes and diatoms were mainly present in the subantarctic water west of Tasmania (Stn 2). In the W-SAZ (Stn 4), haptophytes, and green algae (Chl*b*) dominated in surface water; some cyanobacteria (zeaxanthin and Chl*b*) and diatoms were also present at 50 m. At the depth of total Chl*a* maximum, small diatoms, and haptophytes dominated in the PFZ, whereas cyanobacteria and diatoms dominated in the E-SAZ. Peridinin was only significantly present in the E-SAZ (data not shown), representing 24 and 8% of large and small phytoplankton Chl*a*, respectively. Prasinoxanthin was only present at marginal levels (1% of Chl*a*) at Stns 12 and 17 (data not shown).
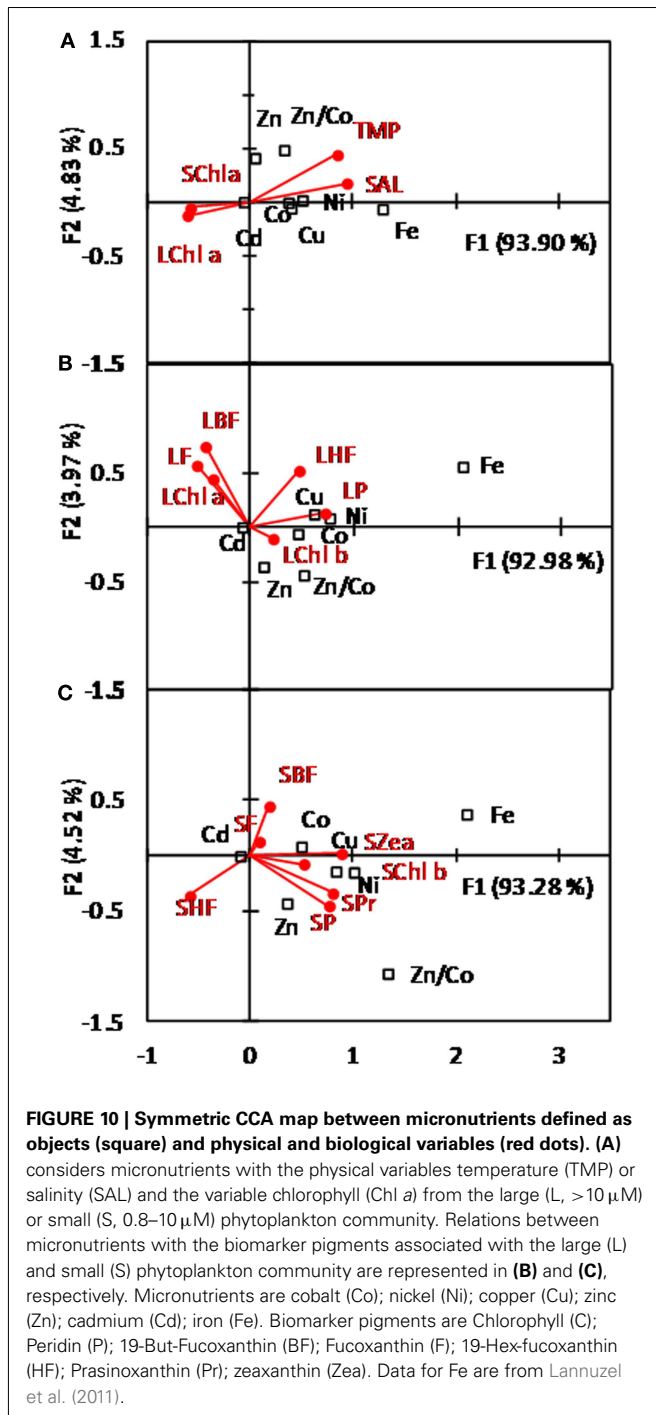
The use of CHEMTAX revealed that, except for prasinophytes, representing up to 35% of the large and small phytoplankton in the W-SAZ, the composition of the phytoplankton community calculated by CHEMTAX was similar in the W-SAZ and the PFZ (**Figures 9A,B**). In these two zones, large phytoplankton were dominated by diatoms, whereas small phytoplankton were dominated by haptophytes. Dinoflagellates were present in both phytoplankton size fractions, representing 10–30% of the phytoplankton community. In the E-SAZ, the composition of the phytoplankton community inferred by CHEMTAX was more complex

FIGURE 9 | Estimation of the phytoplankton community using CHEMTAX per de Salas et al. (2011). The major groups composing the small (S, 0.8–10 µm) and large (L, >10 µm) phytoplankton communities are represented in percent (stacked bars) at different depths for stations in the E-SAZ [Stn 4 **(A)**], PFZ [Stn 6 **(B)**], and W-SAZ [Stn 17 **(C)**].

(**Figure 9C**). In the phytoplankton bloom (top 40 m, **Figure 6**), diatoms are only marginal (10%, **Figure 9C**), likely due to Si depletion. Large phytoplankton are mainly composed of dinoflagellates and haptophytes (40% each), whereas small phytoplankton mainly contained dinoflagellates (37%), and cyanobacteria (30%), with some haptophytes (18%) and prasinophytes (14%).

STATISTICAL CORRELATIONS OF NUTRIENTS WITH PHYSICAL AND BIOLOGICAL PARAMETERS

Canonical correspondence analysis representation of micronutrients according to temperature, salinity, small, and large phytoplankton Chl*a* (**Figure 10A**, 0–100 m), demonstrated four micronutrient "clusters", with Fe being closer to physical parameters and Cd closer to Chl*a*. The other micronutrients were intermediately located with Cu, Co, and Ni closer to physical parameters and Zn closer to Chl*a*. These data were also supported by the Pearson's correlation tests (**Table A1** in Appendix). Indeed, Fe was the only micronutrient to significantly positively correlate with temperature and salinity but not significantly with NO_x and PO_4. No significant correlation between micronutrients and silicic acid were obtained. Co, Cu, Ni, Cd, and Zn were significantly

FIGURE 10 | Symmetric CCA map between micronutrients defined as objects (square) and physical and biological variables (red dots). (A) considers micronutrients with the physical variables temperature (TMP) or salinity (SAL) and the variable chlorophyll (Chl *a*) from the large (L, >10 μM) or small (S, 0.8–10 μM) phytoplankton community. Relations between micronutrients with the biomarker pigments associated with the large (L) and small (S) phytoplankton community are represented in **(B)** and **(C)**, respectively. Micronutrients are cobalt (Co); nickel (Ni); copper (Cu); zinc (Zn); cadmium (Cd); iron (Fe). Biomarker pigments are Chlorophyll (C); Peridin (P); 19-But-Fucoxanthin (BF); Fucoxanthin (F); 19-Hex-fucoxanthin (HF); Prasinoxanthin (Pr); zeaxanthin (Zea). Data for Fe are from Lannuzel et al. (2011).

positively inter-correlated and all negatively correlated with Fe. Fe was also significantly negatively correlated to ratio dZn/dCo (**Table A1** in Appendix).

No statistically significant Pearson's coefficient of correlation was observed between micronutrients and Chl*a* throughout the study region (total, large, and small phytoplankton, **Table A1** in Appendix). However, the degree of significance of positive correlation followed the order Cd > Zn > Ni, Cu, Co, with Ni and Cu more related to small phytoplankton Chl*a*. Fe was only weakly

correlated (−0.1) to Chl*a*. These correlations are represented for Cd, Zn, Co, and Fe in **Figure 11**. Data from the depths of Chl*a* maximum (labeled as "*" in **Figures 11A–F**) significantly deviated from dCd/Chl*a* and dZn/Chl*a* relations. Exclusion of these points, resulted in a significant correlation between dissolved Cd and Zn with total, small, and large Chl*a* concentrations. No correlation was observed between Co, Fe, and Chl*a* (**Figures 11G–L**).

Canonical correspondence analysis representations of micronutrients with large (L- **Figure 10B**) and small (S- **Figure 10C**) phytoplankton biomarker pigments confirmed that Fe was poorly related to phytoplankton. Fe was closest to L-peridinin and S-zeazanthin, the only two pigments for which a significant positive correlation was obtained (**Table A1** in Appendix), suggesting that Fe could affect the dynamics of dinoflagellates and cyanobacteria in the E-SAZ. Cd was the micronutrient that was the most closely related to all biomarker pigments (**Figures 10B,C**), whereas Cu and Ni formed a cluster closely related to L-peridinin, L-hex-fucoxanthin, and S-zeazanthin, S-prasioxanthin, S-Chl*b*, and S-peridinin. Co and Zn were differentiated by Co being closer to L-peridinin and L-Chl*b*, S-fucoxanthin, S-but-fucoxanthin, S-Chl*b* and S-zeazanthin, and Zn being closer to L-Chl*b* and S-peridinin, S-prasinoxanthin and S-Chl*b*. The ratio dZn/dCo was more associated with biomarker pigments from large rather than small phytoplankton. Co, Ni, Cu, and Cd were statistically positively correlated with L-but-fucoxanthin, L-fucoxanthin, and negatively correlated to S-Chl*b*. Co was also significantly negatively correlated to S-zeaxanthin. Zn is only significantly positively correlated with Shex-fucoxanthin and dZn/dCo to L-hex-fucoxanthin (**Table A1** in Appendix). Pearson's correlation tests also showed significant positive correlations between NO_x and PO_4 with L-but-fucoxanthin and L-fucoxanthin, between Si and S-fucoxanthin, and between nitrite (NO_2) and S-hex-fucoxanthin (**Table A1** in Appendix).

DISCUSSION

Previous studies from the SAZ-Sense project have demonstrated that the E-SAZ, despite greater Chl*a* was less productive than the W-SAZ at the time of observation (Cavagna et al., 2011; Westwood et al., 2011; **Table A1** in Appendix). Biomarker pigments and CHEMTAX analysis showed a contrasted phytoplankton community in the study region. Distribution of phytoplankton size classes and dominant groups accorded with microscopic observations, pigment size class, and CHEMTAX calculations done during the SAZ-Sense voyage (de Salas et al., 2011; Pearce et al., 2011). There is, therefore, a clear difference between these two SAZ regions.

Our distribution of micronutrients agreed with previous studies in the region (Ellwood, 2008; Lai et al., 2008). Similar hydrology for these studies, despite the difference in season and location (winter and eastwards of the SAZ-Sense study for Ellwood, 2008), allow a comparison of the distribution of micronutrients. Similar Cd, Cu, and Ni distribution in the SAZ, closely related to PO_4 (see **Figure 5**), suggested that this distribution of micronutrients, is the result of long term processes (seasonal and longer – see also Butler et al., in revision). Co, too, was closely related to PO_4 in the top 150–200 m and with a distribution that tracks with timescales of seasonal or longer. Deeper in the SAZ water column, Co is known to display scavenged characteristics, and is strongly
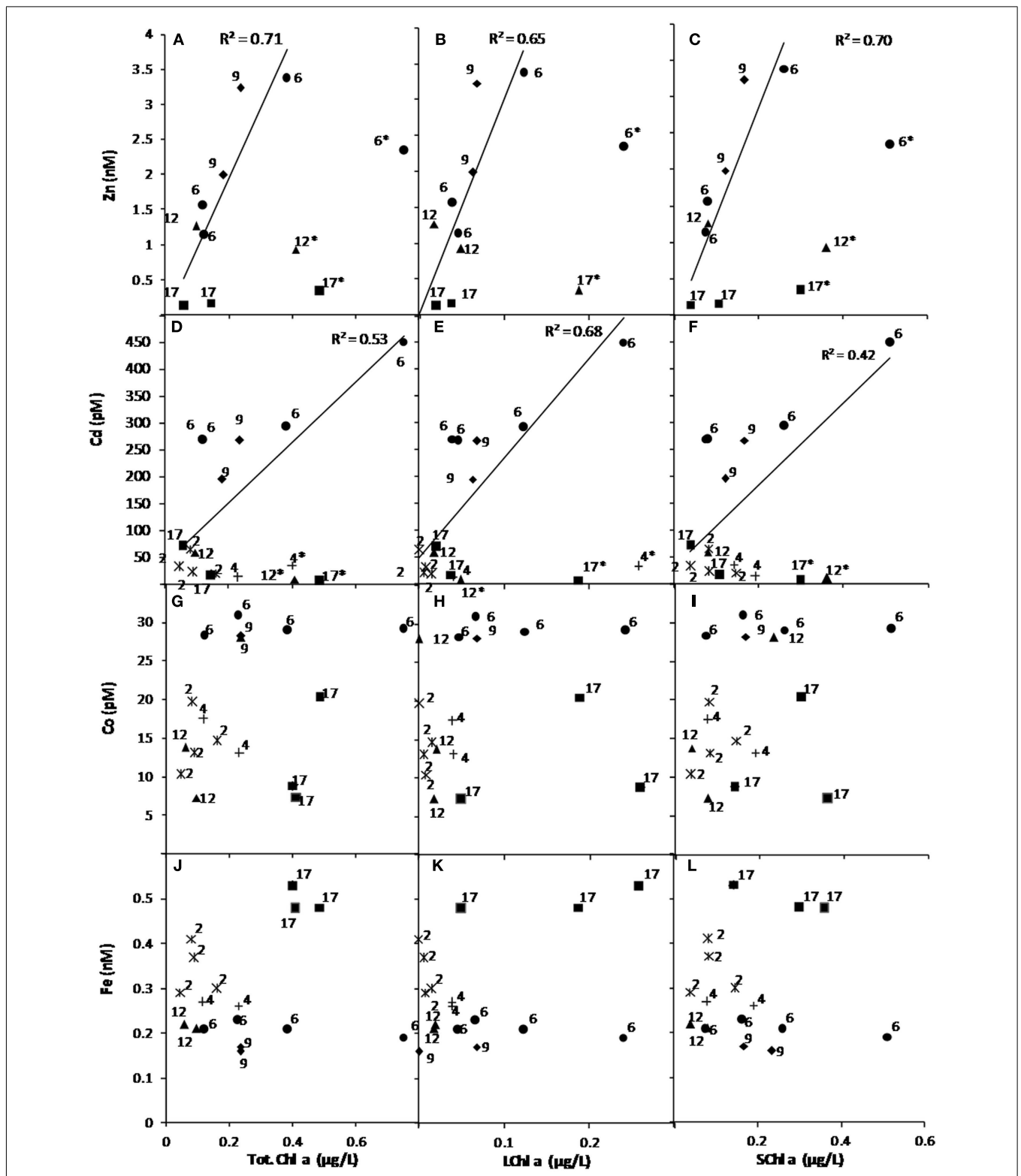
FIGURE 11 | Relation between dissolved micronutrients and chlorophyll *a* associated with the total [Chl*a*, (A), (D), (G), (J)], large [LChl*a*, >10 μm, (B), (E), (H), (K)], and small [SChl*a*, 0.8–10 μm, (C), (F), (I), (L)] phytoplankton communities. Relationships are shown for Zn (A–C), Cd (D–F), Co (G–I) and Fe (J–L) and coefficient of correlation are given when significant relationships were found (Zn and Cd only). Each station has been represented using a different symbol and the station labeled with " *" correspond to depth with a maximum of Chl*a* and were removed to obtain a significant correlation for Cd and Zn. Fe data are from Lannuzel et al. (2011).

influenced by concentrating processes in the Antarctic Zone (seen to some degree here at Stns 6, 9, and 10) and intermediate water formation (Butler et al., submitted). By comparison, the dissolved iron distribution resulted from short term processes, involving a rapid recycling, episodic dust input, and intrusion of oligotrophic subtropical water into the SAZ region, generating a patchy distribution of dissolved iron (Bowie et al., 2009, 2011a,b; Lannuzel et al., 2011; Mongin et al., 2011). Butler et al. (in revision) have also proposed that distribution of Zn in SAZ-E waters was modulated by short term processes at the time of the SAZ-Sense voyage, although it was quite unlike that of Fe, which is supported by their lack of correlation reported here. The patchiness of Fe and Zn at SAZ-E results from region being dominated by the East Australian Current eddy field, the different supply mechanisms for the two pivotal metals, and the ensuing sub-mesoscale irregularities in phytoplankton productivity

Determination of the control by the full suite of micronutrients (Fe, Zn, and other transition metals) on phytoplankton biomass and community structure is, thus, first step to elucidate how primary productivity and the balance between carbon export and recycling are controlled. However, the identification of the nutritive status (e.g., limited, co-limited, replete) of *in situ* phytoplankton communities is a major challenge. Statistical analyses of the relationship between micronutrients and phytoplankton, revealed complex heterogeneous relationships in which all micronutrients (Fe, Zn, Cd, Co, Cu, and Ni) are important for specific phytoplankton groups. All the micronutrients studied were depleted in surface waters and presented good correlations with dissolved PO_4 (except Fe), demonstrating their nutritive role in phytoplankton growth. The role of micro-nutrients in shaping the phytoplankton community can be further explored by comparing their disappearance ratios in reference to PO_4 with the dissolved metal spot ratios, with previously reported phytoplankton cellular quotas and biological requirements (e.g., Sunda and Huntsman, 1995a,b; Ho et al., 2003; Finkel et al., 2007; Saito et al., 2010; Croot et al., 2011).

In surface water, a greater disappearance ratio is often associated with a greater relative biological uptake but could also be related to differential recycling and remineralization. Several studies have reported a "kink" in the disappearance ratio for Cd which, despite a poor understanding of the mechanisms at play, can be related to a decreased phytoplankton growth rate or "biodilution effect" (Sunda and Huntsman, 2000; Cullen et al., 2003). It is, thus, not surprising that, in the CCA, Cd was the closest to total Chl*a* and to most of the biomarker pigments. Cadmium was the most depleted micronutrient in surface waters (from comparison with concentrations at 150–200 m depth – see Bowie et al., 2011b) and it also showed significant correlation with several biomarker pigments. The disappearance ratio for Cd observed here was slightly lower than for the Ross Sea and the subarctic Pacific (**Table 3**).

In this study, kinks in disappearance ratios were observed for NO_x, Zn, and Cd. The kinks observed for NO_x and Cd correspond to the surface water (25–50 m) of the W- and E-SAZ (Stns 2,4, and 17) but the kink observed for Zn extends deeper at these stations and further south to Stns 5 and 12, suggesting a complex control on phytoplankton growth rate in the region. This is emphasized by the fact that inter-station disappearance ratio is variable and follows a general pattern, where disappearance ratios are increasing southwards with a loss of correlation in the PFZ. Such loss of correlation

could be due to nutrients supply from Upper Circumpolar Deep Water sufficient to swamp the imprint of biological uptake. On the other hand, the disappearance ratio for NO_x is lower in the PFZ. In the Southern Ocean, such a poleward increase in disappearance ratio was recently reported for Zn (Croot et al., 2011), whereas a lower dNO_x/PO_4 was reported in the PFZ and southwards (Levitus et al., 1993; de Baar et al., 1997). These observations were attributed to variation in phytoplankton growth rate and specific phytoplankton uptake ratio (de Baar et al., 1997; Arrigo et al., 1999; Croot et al., 2011). Parameters usually discussed as a control in phytoplankton growth rate with impact on disappearance ratios in the region are (i) iron limitation (e.g., Martin et al., 1990; de Baar et al., 1997; Cullen et al., 2003; Twining et al., 2004a,b; Croot et al., 2011), (ii) combined effect of micronutrients (Sunda and Huntsman, 2000; Twining et al., 2004b; Cullen and Sherrell, 2005), and (iii) community structure (e.g., Sunda and Huntsman, 1995b, 2000; de Baar et al., 1997; Arrigo et al., 1999; Ho et al., 2003; Quigg et al., 2003; Twining et al., 2004a,b; Finkel et al., 2010). It is to be noted that the dependency of disappearance ratios on growth rate and iron addition is not an invariant attribute; it can differ between phytoplankton groups and micronutrients (e.g., Twining et al., 2004b; Finkel et al., 2007). Finally, the effects of light and temperature have also to be considered (Finkel et al., 2007, 2010; Croot et al., 2011).

Comparison of the distribution of the Chl*a* (**Figure 6**) with the depths of the euphotic zone and the mixed layer (**Table A1** in Appendix) allows discussion of the impact of light limitation. In both the W-SAZ and PFZ, most of the Chl*a* is found at the bottom of the euphotic layer, just below the MLD. This clearly illustrates a trade-off between light and nutrient limitation at these sites. In the E-SAZ, light might constrain the bloom in surface waters (Mongin et al., 2011; Westwood et al., 2011; **Table A1** in Appendix), but phytoplankton found in the top 16 m are not light limited. Temperature is known to exert a control in the growth of cyanobacteria (Li, 1998) and can, thus, curtail their extension southwards. However, temperature cannot account for the absence of cyanobacteria in the W-SAZ. In addition, as previously noted, it is likely that phytoplankton present at these high latitudes are well adapted to low temperatures (e.g., Croot et al., 2002). Therefore, it is not expected that temperature acts as a fundamental control of phytoplankton growth here.

During SAZ-Sense, Fe, and Si limitation were postulated in the W-SAZ and the PFZ using microscopic observations (Pearce et al., 2011), diatom silification rate (Fripiat et al., 2011), Si*, and Fe* concentrations (Lannuzel et al., 2011), incubation and Fv/Fm (Schoemann et al., unpublished). Interestingly, except for prasinophytes, the composition of the phytoplankton community was similar at these two locations. The lower disappearance ratio for NO_x in the PFZ could be related to diatoms, such as *Fragilariopsis kerguelensis*, present at Stn 9 (de Salas et al., 2011), and iron limitation (de Baar et al., 1997). By comparison, in the E-SAZ, where a less productive but more complex and diverse phytoplankton community prevailed (this study, de Salas et al., 2011), no iron limitation was observed. In the surface waters of the E-SAZ, the decreased dZn/dCo and dZn/dCd likely reflected biological uptake, whereas the increased dFe/dCo and dFe/dZn likely reflected the iron aerosol input (Bowie et al., 2009; Mongin et al., 2011). The dissolved Fe/PO_4 ratio also indicated iron

enrichment in the surface waters of the W-SAZ and E-SAZ. Based on the iron biological requirement for phytoplankton growth (i.e., half saturation constant), the dissolved iron concentrations measured in surface water were indeed enough to sustain the growth of most diatoms (Coale et al., 2003; Sarthou et al., 2005), and the haptophyte genus, *Phaeocystis* (Coale et al., 2003; Sedwick et al., 2007). However, diatoms were a marginal phytoplankton group, and nanoflagellates and dinoflagellates were the most dominant groups in the E-SAZ at the time of study (this study; de Salas et al., 2011; Pearce et al., 2011). Dinoflagellates were previously reported as dominating the phytoplankton community in the SAZ region south of Australia during austral spring and summer (Kopczynska et al., 2001, 2007). Studies of elemental ratios in phytoplankton have demonstrated that optimal iron content, follows the order cyanobacteria > haptophytes ≥ dinoflagellates ≥ diatoms (Ho et al., 2003; Twining et al., 2004b; Finkel et al., 2010) and that iron enrichment favors the growth of diatoms, but also autotrophic and heterotrophic flagellates (e.g., Twining et al., 2004a). In this case, additional iron sources in the E-SAZ might have relieved iron limitation and favored the growth of flagellates and cyanobacteria. Indeed, dissolved iron concentrations were significantly related to L-Peridin (dinoflagellates – type 1) and S-zeaxanthin (cyanobacteria), both biomarkers present only in the E-SAZ. In this case, phytoplankton in the E-SAZ were not iron-limited at the time of sampling; however, iron had an important effect of the phytoplankton community structure in this region.

The extended Redfield ratio based on micronutrient cellular quota from phytoplankton cultures of $P_1Fe_{7.5}Zn_{0.80}Cu_{0.38}Co_{0.19}Cd_{0.21}$ (Ho et al., 2003), suggests that the biological requirement for growth is usually smaller for other micronutrients than for iron. However, a significantly different extended Redfield ratio of $P_1Zn_{5.4}Fe_{1.8}Ni_{0.61}$ was calculated from a field study during the Southern Ocean Iron Experiment (SOFeX, Twining et al., 2004b), suggesting that Zn biological requirement exceeds the requirement for iron. These differences could be related to different water chemistry, light and phytoplankton species as all of these parameters affect cellular quotas (Finkel et al., 2010). In the study region, the concentrations of micronutrients are lower than iron, especially in the SAZ regions, suggesting that they might play a role in controlling phytoplankton growth or community structure.

Cd and Co nutrition in phytoplankton is coupled to Zn nutrition, because Zn can interchange with Cd and Co to support key enzymes, such as the carbonic anhydrase in some (Price and Morel, 1990; Morel et al., 1994; Sunda and Huntsman, 1995a, 2000; Saito and Goepfert, 2008), but not all phytoplankton species (Timmermans et al., 2001). Laboratory studies suggested that Cd, Co, and Zn use the same biological transport system, which is regulated by cellular Zn concentrations for diatoms and coccolithophores (Sunda and Huntsman, 1995a, 2000). Cobalt is associated with vitamin B$_{12}$ which is essential to, but not synthesized by eukaryotic phytoplankton (Saito et al., 2002; Saito and Goepfert, 2008).

The kink observed for dZn/PO$_4$, could be related to the induction of high affinity transporters which are efficient in maintaining a nearly constant cellular Zn concentration despite decreasing free Zn concentrations (Sunda and Huntsman, 1995a). Zn was the only micronutrient for which significant differences in the relation with other macronutrients were observed (**Figure 5**; **Table 3**). In Ellwood (2008), dissolved Zn and PO$_4$ concentrations were not

significantly related in surface waters ($r^2 < 0.001$, 0–100 m, see **Figure A1** in Appendix) but dissolved Zn and Si were strongly related ($r^2 = 91$). Our data suggest a greater role for Zn in phytoplankton nutrition. The lack of dZn/Si relationship observed here (**Figure A2** in Appendix) could be related to diatoms not being the dominant phytoplankton group in the SAZ at the time set of our study (de Salas et al., 2011), likely related to Si depletion and limitation (Fripiat et al., 2011).

Here, the ratios dZn/PO$_4$:dCd/PO$_4$ of 5 and dZn/PO$_4$:dCo/PO$_4$ of 96 (**Table 3**) showed indeed that Zn had an important nutritive role in the study region. The Zn/PO$_4$ measured here is much higher than data previously reported (**Table 3**, except for Croot et al., 2011). The dZn/PO$_4$ ratio observed here ($>0.5\,\mu$M PO$_4$) was close to the cellular ratio for which growth inhibition is observed in *Emiliania huxleyi* (**Table 3**, in absence of Co and Cd, Sunda and Huntsman, 1995a). For a similar Zn^{2+}/Cd^{2+} than the dZn/dCd ratio observed here, the cellular Zn:P ratio in *E. huxleyi* (1494 μmol mol^{-1}; Sunda and Huntsman, 2000) was close to the dZn/PO$_4$ ratio observed. This suggests that Zn was present at concentrations which could limit or co-limit the growth of coccolithophores, even considering Zn-Cd biological substitution. However, in the E-SAZ, the ratios between Zn and Co dissolved concentrations were smaller than 96, suggesting that Co could be important to complement Zn nutrition. The disappearance ratio for Co was smaller than the cellular Co:P ratios under which growth inhibition was observed for diatoms and coccolithophores (**Table 3**), suggesting that phytoplankton in the E-SAZ could be limited or co-limited by Co.

Based on the Pearson's correlation coefficient, dissolved Zn concentrations were related to L-Chl*b*, S-Chl*b*, S-peridinin, and S-prasinoxanthin, biomarker pigments mostly present in the E-SAZ and at depth in the W-SAZ (50 m), suggesting that Zn nutrition is important in these regions. This observation is reinforced by the fact that higher dissolved ecological stoichiometry was observed at Stns 9 and 10 and that data from the depth of the Chl maximum had a Zn and Cd concentration much lower than those predicted from the dZn/Chl*a* and dCd/Chl*a*. Co was significantly related to L-peridinin, L-Chl*b*, S-Chl*b*, S-fucoxanthin, S-but-fucoxanthin, and S-zeaxanthin. Because these biomarker pigments are mainly present in the W-SAZ (Stn 4, 50 m) and in the E-SAZ (Stns 10–17), it suggests that Co could shape the structure of the phytoplankton community in the SAZ region. The effect of Co on S-Chl*b* and S-zeaxanthin is not surprising given that studies have demonstrated a strict Co requirement in cyanobacteria (Sunda and Huntsman, 1995a; Saito et al., 2002). Oceanic prasinophytes and dinoflagellates, the dominating phytoplankton in the SAZ region, have a greater requirement in Zn, Co, and Cd than diatoms (Ho et al., 2003). Laboratory work demonstrated that the haptophyte, *Phaeocystis*, and diatoms prefer Zn to satisfy their growth requirement, while the haptophyte, *E. huxleyi* prefers Co (Sunda and Huntsman, 2000; Saito and Goepfert, 2008). An elevated dZn/dCo ratio, could favor the growth of diatoms and *Phaeocystis* and be a disadvantage for the growth of *E. huxleyi* (Sunda and Huntsman, 1995a; Saito and Goepfert, 2008). In this study, dZn/dCo was more strongly related to hex-fucoxanthin a biomarker for haptophytes and dinoflagellates (type 2), but not significantly related to fucoxanthin. This might be because fucoxanthin is not only present in diatoms, but also in haptophytes, chrysophytes, and

some dinoflagellates (Jeffrey and Wright, 2006). It should be noted that, in the field, the preference for Zn or Co for natural phytoplankton communities remains largely unknown (e.g., Croot et al., 2002).

Iron is also known to affect the biological uptake of other micronutrients (e.g., Cullen et al., 2003; Ho et al., 2003; Twining et al., 2004b; Cullen and Sherrell, 2005). It, therefore, appears that complex interconnections exist between these metals and phytoplankton. In fact, a significant negative correlation for dFe with dZn/dCo and a high coefficient of correlation (although not statistically significant, 0.4) with hex-fucoxanthin, suggest an interaction between Fe, Zn, and Co in the control of the phytoplankton community in the SAZ region.

This study also focuses on other micronutrients for which data are yet limited. Both Cu and Ni had the same pattern of correlations with biomarker pigments; however, little is known of a coupled effect for Cu and Ni on phytoplankton growth. Both these micronutrients were significantly correlated to L-peridinin, S-peridinin, L-hex-fucoxanthin, S-zeaxanthin, S-prasinoxanthin, S-Chl*b*, demonstrating an effect on most major phytoplankton groups, except diatoms. Cu is involved in nitrogen cycling, electron transfer associated with photosynthesis and Fe uptake (Morel et al., 2003; Maldonado et al., 2006), and Ni is involved in urea assimilation and protection against reactive oxygen species (Morel et al., 2003; Dupont et al., 2010). The disappearance ratios for Ni and Cu are close to previously reported values (**Table 3**). Comparison of the dCu/PO_4 with cellular Cu:P ratio for *Thalassiosira oceanica* and *E. huxleyi* (**Table 3**), as well as other oceanic species including dinoflagellates (Cu:P 60–110 μmol:mol, Ho et al., 2003), suggests that Cu was present at an optimal level for the growth of these eukaryotic phytoplankton. For dCu, a relation with PO_4 ($r^2 > 0.75$) was only observed for stations within the W-SAZ and E-SAZ, suggesting a nutrition role in these regions. For Ni, the disappearance ratio measured here (**Table 3**) was also greater than cellular Ni:P ratios for diatoms and flagellates (160–1150 μmol:mol, Twining et al., 2004b), suggesting optimal conditions for growth in the study region.

As a cautionary note, the disappearance ratios used here can be influenced by scavenging processes, surface input, organic complexation, recycling, and remineralization, biological uptake, and drawdown (e.g., Saito et al., 2010; Croot et al., 2011). Recent studies highlighted important differences in Zn organic speciation between the SAZ and the PFZ, with greater inorganic Zn concentration found in the PFZ (e.g., Ellwood, 2004; Baars and Croot, 2011). For micronutrients that are influenced by short time processes (such as Fe), it is expected that this relation (metal to PO_4) will be significantly blurred, and less meaningful. In addition, snapshot studies will invariably fail to represent the dynamic situation between micronutrients and phytoplankton. For example, grazing, recycling, supply, and phytoplankton succession are not considered. During SAZ-Sense, regenerated production exceeded new production (Cavagna et al., 2011) and grazing dilution experiments demonstrated the complexity of the processes at

play with on average 36–37% herbivory, 39–42% bacterivory, and 21–24% cyanobacterivory (Stns 4 and 17; Pearce et al., 2011). Grazing is paramount for nutrient recycling, which was very efficient for Fe in the E-SAZ (Bowie et al., 2009). Nonetheless, our study provides much needed information on the biological relevance of micronutrients, other than iron during the austral summer of 2007. It indicated that Zn, Co, and Cd inter-replacement was influential in the E-SAZ region and that interaction between these micronutrients and Fe needs to be considered. Our results also demonstrated that different phytoplankton size classes and functional groups are related differently to micronutrients, possibly attributed to variable biological requirements for growth. Generally, larger phytoplankton have greater micronutrient requirement for growth (Sarthou et al., 2005; Hassler and Schoemann, 2009; Finkel et al., 2010). Here, L-phyto were not more strongly related to micronutrients than S-phyto, illustrating the complexity at play in the field.

If the E-SAZ, represents the future of the SAZ region, further investigations on the relations among Fe, Cd, Zn, and Co and their ability to shape the structure of the phytoplankton community is required. In addition, effort should be made to increase our knowledge of the micronutrient requirement for dinoflagellates, a dominant group in the E-SAZ. To integrate the key processes at play, ship-board experiments would be required to study the effect of micronutrients on the natural phytoplankton community and measure their requirement for growth (e.g., Coale et al., 2003). Because macro- and micronutrients support biological processes that are interrelated or have synergistic or antagonistic relations, an experimental approach at sea should investigate these complex interactions, rather than focusing on a single element.

REFERENCES

Arrigo, K. R., Robinson, D. H., Worthen, D. L., Dunbar, R. B., DiTullio, G. R., Van Woert, M., and Lizotte, M.

P. (1999). Phytoplankton community structure and the drawdown of nutrients and CO_2 in the Southern Ocean. *Science* 283, 365–367.

Baars, O., and Croot, P. L. (2011). The speciation of dissolved zinc in the Atlantic sector of the Southern Ocean. *Deep Sea Res.*

Part 2 Top. Stud. Oceanogr. 58, 2720–2732.

Banse, K. (1996). Low seasonality of low concentrations of surface

chlorophyll in the Subantarctic water ring: underwater irradiance, iron, or grazing? *Prog. Oceanogr.* 37, 241–291.

Biller, D. V., and Bruland, K. W. (2012). Analysis of Mn, Fe, Co, Ni, Cu, Zn, Cd, and Pb in seawater using the Nobias-chelate PA1 resin and magnetic sector inductively coupled plasma mass spectrometry (ICP-MS). *Mar. Chem.* 130–131, 12–20.

Bowie, A. R., Lannuzel, D., Remenyi, T. A., Wagener, T., Lam, P. J., Boyd, P. W., Guieu, C., Townsend, A. T., and Trull, T. W. (2009). Biogeochemical iron budgets of the Southern Ocean south of Australia: decoupling of iron and nutrient cycles in the subantarctic zone by the summertime supply. *Global Biogeochem. Cycles* 23, GB4034.

Bowie, A. R., Trull, T. W., Griffiths, F. B., and Dehairs, F. (2011a). Estimating the sensitivity of the subantarctic zone to environmental change: the SAZ-Sense project. *Deep Sea Res. Part II Top. Stud. Oceanogr.* 58, 2051–2058.

Bowie, A. R., Griffiths, F. B., Dehairs, F., and Trull, T. W. (2011b). Oceanography of the subantarctic and polar frontal zones south of Australia during summer: setting for the SAZ-Sense study. *Deep Sea Res. Part 2 Top. Stud. Oceanogr.* 58, 2059–2070.

Bruland, K. W. (1980). Oceanographic distributions of cadmium, zinc, nickel and copper in the North Pacific. *Earth Planet. Sci. Lett.* 47, 176–198.

Buitenhuis, E., Timmermans, K. R., and de Baar, H. J. W. (2003). Zinc-bicarbonate colimitation of Emilianiahuxleyi. *Limnol. Oceanogr.* 48, 1575–1582.

Cavagna, A. J., Elskens, M., Griffiths, F. B., Fripiat, F., Jacquet, S. H. M., Westwood, K. J., and Dehairs, F. (2011). Contrasting regimes of production and potential for carbon export in the Sub-Antarctic and Polar Frontal Zones south of Tasmania. *Deep Sea Res. Part 2 Top. Stud. Oceanogr.* 58, 2235–2247.

Coale, K. H., Wang, X., Tanner, S. J., and Johnson, K. S. (2003). Phytoplankton growth and biological response to iron and zinc addition in the Ross Sea and Antarctic Circumpolar Current along 170°W. *Deep Sea Res. Part 2 Top. Stud. Oceanogr.* 50, 653–653.

Croot, P. L., Baars, O., and Streu, P. (2011). The Distribution of zinc in the Atlantic sector of the Southern Ocean. *Deep Sea Res. Part 2 Top. Stud. Oceanogr.* 58, 2707–2719.

Croot, P. L., Karlson, B., Wulff, A., Linares, F., and Andersson, K.
(2002). Trace metal/phytoplankton interactions in the skagerrak. *J. Mar. Syst.* 35, 39–60.

Cullen, J. T., Chase, Z., Coale, K. H., Fitzwater, S. E., and Sherrell, R. M. (2003). Effect of iron limitation on the cadmium to phosphorous ratio of natural phytoplankton assemblages from the Southern Ocean. *Limnol. Oceanogr.* 48, 1079–1087.

Cullen, J. T., and Sherrell, R. M. (2005). Effects of dissolved carbon dioxide, zinc, and manganese on the cadmium to phosphorus ratio in natural phytoplankton assemblages. *Limnol. Oceanogr.* 50, 1193–1204.

de Baar, H. J. W., van Leeuwe, M. A., Scharek, R., Goeyens, L., Bakker, K. M. J., and Fritsche, P. (1997). Nutrient anomalies in Fragilariopsiskerguelensis blooms, iron deficiency and the nitrate/phosphate ratio (A. C. Redfield) of the Antarctic Ocean. *Deep Sea Res. Part 2 Top. Stud. Oceanogr.* 44, 229–260.

de Salas, M. F., Eriksen, R., Davidson, A. T., and Wright, S. W. (2011). Protistan communities in the Australian sector of the Sub-Antarctic zone during SAZ-Sense. *Deep Sea Res. Part 2 Top. Stud. Oceanogr.* 58, 2135–2149.

Dupont, C. L., Barbeau, K., and Palenik, B. (2008). Ni limitation and uptake in marine Synechococcus. *Appl. Environ. Microbiol.* 74, 23–31.

Dupont, C. L., Buck, K. N., Palenik, B., and Barbeau, K. (2010). Nickel utilization in phytoplankton assemblages from contrasting oceanic regimes. *Deep Sea Res. Part 2 Top. Stud. Oceanogr.* 57, 553–566.

Ebersbach, F., Trull, T. W., Davies, D. M., and Bray, S. G. (2011). Controls on mesopelagic particle fluxes in the Sub-Antarctic and Polar Frontal Zones in the Southern Ocean south of Australia in summer – perspectives from free-drifting sediment traps. *Deep Sea Res. Part 2 Top. Stud. Oceanogr.* 58, 2260–2276.

Ellwood, M. J. (2004). Zinc and cadmium speciation in subantarctic waters east of New Zealand. *Mar. Chem.* 87, 37–58.

Ellwood, M. J. (2008). Wintertime trace metal (Zn, Cu, Ni, Cd, Pb and Co) and nutrient distributions in the subantarctic zone between 40–52°S; 155–160°E. *Marine Chem.* 112, 107–117.

Ellwood, M. J., van den Berg, C. M. G., Boye, M., Veldhuis, M., Jong, J. T. M., de Baar, H. J. W., de Croot, P. L., and Kattner, G. (2005). Organic
complexation of cobalt across the Antarctic Polar Front. *Mar. Freshw. Res.* 56, 1069–1075.

Finkel, Z. V., Beardall, J., Flynn, K. J., Quigg, A., Rees, T. A. V., and Raven, J. A. (2010). Phytoplankton in a changing world: cell size and elemental stoichiometry. *J. Plankton Res.* 32, 119–137.

Finkel, Z. V., Quigg, A. S., Chiampi, R. K., Schofield, O. E., and Falkowski, P. G. (2007). Phylogenetic diversity in cadmium: phosphorus ratio regulation by marine phytoplankton. *Limnol. Oceanogr.* 52, 1131–1138.

Fitzwater, S. E., Johnson, K. S., Gordon, R. M., Coale, K. H., and Smith, W. O. Jr. (2000). Trace metal concentrations in the Ross Sea and their relationship with nutrients and phytoplankton growth. *Deep Sea Res. Part 2 Top. Stud. Oceanogr.* 47, 3159–3179.

Fripiat, F., Leblanc, K., Elskens, M., Cavagna, A. J., Armand, L., André, L., Dehairs, F., and Cardinal, D. (2011). Efficient silicon recycling in summer in both the Polar Frontal and Subantarctic Zones of the Southern Ocean. *Mar. Ecol. Prog. Ser.* 435, 33–45.

Hassler, C. S., and Schoemann, V. (2009). Bioavailability of organically bound Fe to model phytoplankton of the Southern Ocean. *Biogeosciences* 6, 2281–2296.

Hassler, C. S., Schoemann, V., Mancuso Nichols, C. A., Butler, E. C. V., and Boyd, P. W. (2011). Saccharides enhance iron bioavailability to southern ocean phytoplankton. *Proc. Natl. Acad. Sci. U.S.A.* 108, 1076–1081.

Herraiz Borreguero, L., and Rintoul, S. R. (2011). Regional circulation and its impact on upper ocean variability south of Tasmania. *Deep Sea Res. Part 2 Top. Stud. Oceanogr.* 58, 2071–2081.

Hill, K. S., Rintoul, S. R., Coleman, R., and Ridgway, K. R. (2008). Wind forced low frequency variability of the East Australia Current. *Geophys. Res. Lett.* 35, L08602.

Ho, T. Y., Quigg, A., Finkel, Z. V., Milligan, A. J., Wyman, K., Falkowski, P. G., and Morel, F. M. M. (2003). The elemental composition of some marine phytoplankton. *J. Phycol.* 39, 1145–1159.

Jacquet, S. H. M., Lam, P. J., Trull, T. W., and Dehairs, F. (2011). Carbon export production in the Sub-Antarctic zone and Polar Front Zone south of Tasmania. *Deep Sea Res. Part 2 Top. Stud. Oceanogr.* 58, 2277–2292.
Jeffrey, S. W., and Vesk, M. (1997). "Introduction to marine phytoplankton and their pigment signatures", in *Phytoplankton Pigments in Oceanography: Guidelines to Modern Methods*, eds S. W. Jeffrey, R. F. C. Mantoura, and S. W. Wright (Paris: UNESCO Publishing), 37–84.

Jeffrey, S. W., and Wright, S. W. (2006). "Photosynthetic pigments in marine microalgae: insights from cultures and the sea", in *Algal Cultures, Analogues of Blooms and Applications*, ed. D. V. Subba Rao (Enfield, NH: Science Publishers), 33–90.

Kidston, M., Matear, R., and Baird, M. E. (2011). Parameter optimization of a marine ecosystem model at two contrasting stations in the sub-Antarctic zone. *Deep Sea Res. Part 2 Top. Stud. Oceanogr.* 58, 2301–2315.

Kopczynska, E., Savoye, N., Dehairs, F., Cardinal, D., and Elskens, M. (2007). Spring phytoplankton assemblages in the Southern Ocean between Australia and Antarctica. *Polar Biol.* 31, 77–88.

Kopczynska, E. E., Dehairs, F., Elskens, M., and Wright, S. (2001). Phytoplankton and microzooplankton variability between the Subtropical and Polar Fronts south of Australia: thriving under regenerative and new production in late summer. *J. Geophys. Res.* 106, 31597–31609.

Lai, X., Norisuye, K., Mikata, M., Minami, T., Bowie, A. R., and Sohrin, Y. (2008). Spatial and temporal distribution of Fe, Ni, Cu and Pb along 140°E in the Southern Ocean during austral summer 2001/02. *Mar. Chem.* 111, 171–183.

Lane, T. W., Saito, M. A., George, G. N., Pickering, I. J., Prince, R. C., and Morel, F. M. (2005). A cadmium enzyme from a marine diatom. *Nature* 435, 42.

Lannuzel, D., Remenyi, T., Lam, P. J., Townsend, A., Ibisanmi, E., Butler, E., Wagener, T., Schoemann, V., and Bowie, A. R. (2011). Distributions of dissolved and particulate iron in the Sub-Antarctic and Polar Frontal Southern Ocean (Australian sector). *Deep Sea Res. Part 2 Top. Stud. Oceanogr.* 58, 2094–2112.

Levitus, S., Conkright, M. E., Reid, J. L., Najjar, R. G., and Mantyla, A. (1993). Distribution of nitrate, phosphate and silicate in the world oceans. *Prog. Oceanogr.* 31, 245–273.

Li, W. K. W. (1998). Annual average abundance of heterotrophic bacteria and Synechococcus in surface ocean waters. *Limnol. Oceanogr.* 43, 1745–1753.

Lohan, M. C., Crawford, D. W., Purdie, D. A., and Statham, P. J. (2005). Iron and zinc enrichment in the north eastern subarctic Pacific: ligand production and zinc bioavailability in response to phytoplankton growth. *Limnol. Oceanogr.* 50, 1427–1437.

Lohan, M. C., Statham, P. J., and Crawford, D. W. (2002). Total dissolved Zinc in the upper water column of the subarctic North east Pacific. *Deep Sea Res. Part 2 Top. Stud. Oceanogr.* 24–25, 5793–5808.

Maldonado, M. T., Allen, A. E., Chong, J. S., Lin, K., Leus, D., Karpenko, N., and Harris, S. L. (2006). Copper-dependent iron transport in coastal and oceanic diatoms. *Limnol. Oceanogr.* 51, 1729–1743.

Martin, J. H., Gordon, R. M., and Fitzwater, S. E. (1990). Fe in Antarctic waters. *Nature* 345, 156–158.

Martin, J. H., Gordon, R. M., Fitzwater, S. E., and Broenkow, W. W. (1989). VERTEX: phytoplankton/iron studies in the Gulf of Alaska. *Deep Sea Res. Part 2 Top. Stud. Oceanogr.* 36, 649–680.

McNeil, B. I., Tillbrook, B., and Matear, R. J. (2001). Accumulation and uptake of anthropogenic CO_2 in the Southern Ocean, south of Australia between 1968 and 1996. *J. Geophys. Res.* 106, C12.

Metzl, N., Tillbrook, B., and Poisson, A. (1999). The annual fCO_2 cycle and the air-sea CO_2 flux in the sub-Antarctic ocean. *Tellus B Chem. Phys. Meteorol.* 51B, 849–861.

Moffett, J. W., and Brand, L. E. (1996). Production of strong extracellular Cu chelators by marine cyanobacteria in response to Cu stress. *Limnol. Oceanogr.* 41, 388–395.

Mongin, M., Matear, R., and Chamberlain, M. (2011). Seasonal and spatial variability of remotely sensed chlorophyll and physical fields in the SAZ-Sense region. *Deep Sea Res. Part 2 Top. Stud. Oceanogr.* 58, 2082–2093.

Morel, F. M. M., Milligan, A. J., and Saito, M. A. (2003). Marine bioinorganic chemistry: the role of trace of metals in the oceanic cycles of major nutrients. *Treatise Geochem.* 6, 113–143.

Morel, F. M. M., and Price, N. M. (2003). The biogeochemical cycles of trace metals in the oceans. *Science* 300, 944–947.

Morel, F. M. M., Reinfelder, J. R., Roberts, S. B., Chamberlain, C. P., Lee, J. G., and Yee, D. (1994). Zinc and carbon co-limitation of marine phytoplankton. *Nature* 369, 740–742.

Pearce, I., Davidson, A. T., Thomson, P., Wright, S. W., and van den Enden, R. (2011). Marine microbial ecology in the Sub-Antarctic Zone: rates of bacterial and phytoplankton growth and grazing by heterotrophic protists. *Deep Sea Res. Part 2 Top. Stud. Oceanogr.* 58, 2248–2259.

Price, N. M., and Morel, F. M. M. (1990). Cd and Co substitution for Zn in a marine diatom. *Nature* 344, 658–660.

Quigg, A., Finkel, Z. V., Irwin, A. J., Rosenthal, Y., Ho, T. Y., Reinfelder, J. R., Schofield, O., Morel, F. M. M., and Falkowski, P. G. (2003). The evolutionary inheritance of elemental stoichiometry in marine phytoplankton. *Nature* 425, 291–294.

Quigg, A., Irwin, A. J., and Finkel, Z. V. (2011). Evolutionary inheritance of elemental stoichiometry in phytoplankton, *Proc. R. Soc. B Biol. Sci.* 278, 526–534.

Redfield, A. C., Ketchum, B. H., and Richards, F. A. (1963). "The influence of organisms on the composition of sea-water", in *The Composition of Seawater. Comparative and Descriptive Oceanography. The Sea: Ideas and Observations on Progress in the Study of the Seas*, Vol. 2, ed. M. N. Hill (New York, NY: Interscience), 26–77.

Ridgway, K. R. (2007). Seasonal circulation around Tasmania: an interface between eastern and western boundary dynamics. *J. Geophys. Res.* 112, C10016.

Rintoul, S. R., and Trull, T. W. (2001). Seasonal evolution of the mixed layer in the Subantarctic Zone, south of Australia. *J. Geophys. Res.* 106, 31447–31462.

Rosenberg, M. (2007). *Saz-Sense, Marine Science Cruise Au0703 – Oceanographic Field Measurements and Analysis*. unpublished report, Ace Cooperative Research Centre. Hobart, TAS, 23.

Saito, M. A., and Goepfert, T. J. (2008). Zinc-cobalt colimitation in Phaeocystis Antarctica. *Limnol. Oceanogr.* 53, 266–275.

Saito, M. A., Goepfert, T. J., Noble, A. E., Sedwick, P. N., and DiTullio, G. R. (2010). A seasonal study of dissolved cobalt in the Ross Sea of Antarctica: micronutrient control, absence of observed scavenging, and relationships with Zn, Cd, and P. *Biogeosciences* 7, 4059–4082.

Saito, M. A., Goepfert, T. J., and Ritt, J. T. (2008). Some thoughts on the concept of co-limitation: three definitions and the importance of bioavailability. *Limnol. Oceanogr.* 53, 276–290.

Saito, M. A., and Moffett, J. W. (2001). Complexation of cobalt by natural organic ligands in the Sargasso Sea as determined by a new high-sensitivity electrochemical cobalt speciation method suitable for open ocean work. *Mar. Chem.* 75, 49–68.

Saito, M. A., Moffett, J. W., Chisholm, S. W., and Waterbury, J. B. (2002). Cobalt uptake in Prochlorococcus. *Limnol. Oceanogr.* 47, 1629–1636.

Sarthou, G., Timmermans, K., Blain, S., and Tréguer, P. (2005). Growth physiology and fate of diatoms in the ocean: a review. *J. Sea Res.* 53, 25–42.

Schlitzer, R. (2012). *Ocean Data View (version 4.5)*. Available at: http://odv.awi.de

Sedwick, P. N., Garcia, N. S., Riseman, S. F., Marsay, C. M., and DiTullio, G. R. (2007). Evidence for high iron requirements of colonial *Phaeocystis antarctica* at low irradiance. *Biogeochemistry* 83, 83–97.

Shelley, R. U., Zachhuber, B., Sedwick, P. N., Worsfold, P. J., and Lohan, M. C. (2010). Determination of total dissolved cobalt in UV-irradiated seawater using flow injection with chemiluminescence detection. *Limnol. Oceanogr. Methods* 8, 352–362.

Sokolov, S., and Rintoul, S. R. (2002). Structure of Southern Ocean fronts at 140°E. *J. Mar. Syst.* 37, 151–184.

Sunda, W. G., and Huntsman, S. A. (1995a). Regulation of copper concentration in the oceanic nutricline by phytoplankton uptake and regeneration cycles. *Limnol. Oceanogr.* 40, 132–137.

Sunda, W. G., and Huntsman, S. A. (1995b). Cobalt and zinc interreplacement in marine phytoplankton: biological and biogeochemical implications. *Limnol. Oceanogr.* 40, 1404–1407.

Sunda, W. G., and Huntsman, S. A. (2000). Effect of Zn, Mn, and Fe on Cd accumulation in phytoplankton: implications for oceanic Cd cycling. *Limnol. Oceanogr.* 45, 1501–1516.

Timmermans, K. R., Snoek, J., Gerringa, L. J. A., Zondervan, I., and de Baar, H. J. W. (2001). Not all eukaryotic algae can replace zinc with cobalt: Chaetoceros Calcitrans (Bacillariophyceae) versus Emilianiahuxleyi (Prymnesiophyceae). *Limnol. Oceanogr.* 46, 699–703.

Toggweiler, J. R., and Russell, J. (2008). Ocean circulation in a warming climate. *Nature* 451, 286–288.

Trull, T. W., Rintoul, S. R., Hadfield, M., and Abraham, E. R. (2001). Circulation and seasonal evolution of Polar waters south of Australia: implications for iron fertilisation of the Southern Ocean. *Deep Sea Res. Part II Top. Stud. Oceanogr.* 48, 2439–2466.

Twining, B. S., Baines, S. B., Fisher, N. S., and Landry, M. R. (2004a). Cellular iron contents of plankton during the Southern Ocean Iron Experiment (SOFeX). *Deep Sea Res. Part II Top. Stud. Oceanogr.* 51, 1827–1850.

Twining, B. S., Baines, S. B., and Fisher, N. S. (2004b). Element stoichiometries of individual plankton cells collected during the Southern Ocean Iron Experiment (SOFeX). *Limnol. Oceanogr.* 49, 2115–2128.

van Heukelem, L., and Thomas, C. (2001). Computer assisted high-performance liquid chromatography method development with applications to the isolation and analysis of phytoplankton pigments. *J. Chromatogr. A* 910, 31–49.

Watson, R. J., Butler, E. C. V., Clementson, L. A., and Berry, K. M. (2005). Flow analysis with fluorescence detection for the determination of trace levels of ammonium in seawater. *J. Environ. Monit.* 7, 37–42.

Westwood, K. J., Griffiths, F. B., Webb, J. P., and Wright, S. W. (2011). Primary production in the Sub-Antarctic and Polar Frontal zones south of Tasmania, Australia; SAZ-Sense survey, 2007. *Deep Sea Res. Part II Top. Stud. Oceanogr.* 58, 2162–2178.

Conflict of Interest Statement: The authors declare that the research was conducted in the absence of any commercial or financial relationships that could be construed as a potential conflict of interest.

APPENDIX

Table A1 | Summary of important properties from the W-SAZ (Stn 4), PFZ (Stn 6), and E-SAZ (Stn 9) during the SAZ-Sense study.

Properties	W-SAZ	PFZ	E-SAZ
Euphotic layer depth[1], m	61 ± 5	76 ± 14	47 ± 13
Mixed layer depth[2], m	41 ± 18	53 ± 6	79 ± 2 (16 ± 2)
Integrated Chl a[3]	46.0 ± 11.5	58.8 ± 2.9	62.4 ± 20.0
Gross primary production[4]	93 ± 49	37 ± 7	60 ± 29
Grazing rate[5]	82 ± 38	47 ± 10	67 ± 12
Remineralization rate[6]	2.1 ± 0.4	5.0 ± 1.6	3.7 ± 0.4
Nitrate seasonal depletion[7]	8.9 ± 1.8	8.1 ± 0.4	11.0 ± 1.7
N:P seasonal depletion ratio[8]	16 ± 6	12 ± 1	17 ± 3

[1]*From Westwood et al. (2011),* [2]*Calculated after Rintoul and Trull (2001), a distinct shallow mixed layer depth is shown in bracket for the E-SAZ, see Mongin et al. (2011),* [3]*0–150 m (mg m^{-2}), from Westwood et al. (2011),* [4]*mmol C m^{-2} d^{-1}, from Cavagna et al. (2011),* [5]*% Total Primary Production removed, from Pearce et al. (2011),* [6]*Mesopelagic C remineralization, 100–600 m (mmol C m^{-2} d^{-1}) from Jacquet et al. (2011),* [7]*Mixed layer N depletion uses means from 150 to 200 m depth to represent winter surface values (mmol L^{-1}) from Bowie et al. (2011b),* [8]*Mixed layer N:P ratio uses means from 150 to 200 m depth to represent winter surface values from Bowie et al. (2011b).*

Table A2 | Metal disappearance ratio relative to dissolved phosphate for each station.

Stn #	Latitude (°S)	Longitude (°E)	Co	Zn	Cd	Ni	Cu
2	44.89	143.05	20.4 (0.92)	NA	147 (0.52)	1.52 (1.00)	ND
			11.0 (0.54)		*433 (0.99)*	*1.67 (0.91)*	*0.28 (0.85)*
4	46.32	140.61	13.6 (0.84)	NA	159 (0.74)	1.12 (0.60)	ND
			12.5 (0.58)		*486 (0.96)*	*1.84 (0.95)*	*0.63 (0.95)*
5	48.99	143	106 (0.98)	NA	871 (1.00)	5.50 (0.96)	0.27 (0.76)
			7.02 (0.53)		*379 (0.99)*	*1.70 (0.98)*	*0.31 (0.87)*
6	54.00	145.88	ND	4.73 (0.60)	489 (0.92)	0.73 (0.73)	0.72 (0.71)
			ND	*7.38 (0.86)*	*463 (0.90)*	*1.58 (0.95)*	*1.31 (0.76)*
9	50.87	148.65	ND	ND	ND	ND	−2.55 (0.45)
			79.4 (0.72)	*ND*	*258 (0.67)*	*4.73 (0.40)*	*ND*
10	50.00	149.42	180 (0.42)	8.36 (0.50)	ND	ND	ND
			ND	*7.64 (0.41)*	*931 (0.84)*	*ND*	*ND*
12	48.06	151.20	46.8 (0.90)	5.77 (0.48)	456 (0.97)	1.70 (0.57)	0.62 (0.78)
			59.2 (0.70)	*ND*	*451 (0.76)*	*1.32 (0.64)*	*0.29 (0.34)*
17b	45.55	153.18	20.6 (0.80)	0.99 (0.46)	84.9 (0.86)	1.46 (0.91)	0.35 (0.98)
			5.00 (0.32)	*1.29 (0.59)*	*346 (0.98)*	*1.92 (1.00)*	*0.35 (0.91)*
17j	45.55	153.18	24 (0.73)	0.73 (0.54)	142 (0.86)	1.08 (0.72)	0.24 (0.72)
			6.17 (0.62)	*0.61 (0.83)*	*371 (0.94)*	*1.78 (0.98)*	*0.36 (0.92)*

Disappearance ratios are presented with their coefficient of correlation (r^2, in bracket) for depths between 0 and 100 m (roman font, $n = 4$) and 125–1000 m (italic font, $n = 7$). Disappearance ratio is given in pM/μM for Co, Cd, and Ni, and in nM/μM for Cu and Zn. NA = not applicable due to lack of data, ND = not detected as $r^2 < 0.3$.

Table A3 | Pearson correlation table showing the coefficient of correlation between two parameters considering all stations and all depths (0–125 m).

Variables	T	S	SI	NOx	Ph	A	N	Co	Ni	Cu	Zn	Cd	Fe	Zn/Co	Tot Chl a	LChl a
S	0.92															
SI	0.23	0.27														
NOx	−0.76	−0.75	0.19													
Ph	−0.79	−0.76	−0.28	0.98												
A	−0.29	−0.17	−0.05	0.00	0.12											
N	−0.44	−0.43	−0.32	0.52	0.54	0.45										
Co	−0.90	−0.90	−0.09	0.85	0.85	0.15	0.81									
Ni	−0.97	−0.95	0.07	0.86	0.86	0.15	0.75	0.90								
Cu	−0.93	−0.84	0.15	0.77	0.78	0.25	0.72	0.77	0.91							
Zn	−0.56	−0.68	0.12	0.73	0.84	0.59	0.81	0.72	0.63	0.51						
Cd	−0.96	−0.92	0.08	0.78	0.80	0.13	0.69	0.90	0.93	0.82	0.75					
Fe	0.56	0.73	0.28	−0.51	−0.50	−0.13	−0.71	−0.55	−0.54	−0.40	−0.77	−0.55				
Zn/Co	−0.31	−0.44	−0.08	0.04	0.16	0.64	0.49	0.13	0.14	0.08	0.71	0.23	−0.74			
Tot Chl	−0.66	−0.50	−0.21	−0.14	−0.05	0.60	−0.15	0.14	0.26	0.17	0.30	0.40	−0.14	0.35		
LChl	−0.79	−0.66	−0.26	−0.11	−0.05	0.27	−0.36	0.15	0.19	0.02	0.30	0.35	−0.08	0.12	0.84	
SChl a	−0.56	−0.39	−0.07	−0.12	−0.03	0.66	0.10	0.11	0.27	0.25	0.29	0.38	−0.17	0.45	0.94	0.60

The significance of the correlation is based on the p value ($p > 0.05$) obtained for a 95% confidence interval (data not shown). Values in red are significantly negatively correlated in and values in yellow are significantly positively correlated. The correlation between physical properties (temperature, T, and salinity, S), macronutrients, micronutrients, and the chlorophyll a (Chl a) associated with the total, large (L, $> 10\,\mu m$) and small (S, 0.8–$10\,\mu m$) phytoplankton communities were analyzed. Macronutrients are: silicic acid (SI); $NO_2 + NO_3$ (NOx); phosphate (Ph); ammonia (A); nitrite (N). Micronutrients are: cobalt (Co); nickel (Ni); copper (Cu); zinc (Zn); cadmium (Cd); iron (Fe). Fe data are from Lannuzel et al. (2011).

Table A4 | Pearson correlation table showing the coefficient of correlation between two parameters considering all stations and al depths (0–125 m).

Variables	SI	NOx	Ph	A	N	LP	LBF	LF	LHF	LChl b	SP	SBF	sf	SPr	SHF	SZea
NOx	0.19															
Ph	0.28	0.98														
A	−0.05	0.00	0.12													
N	−0.32	0.52	0.54	0.45												
LP	−0.22	−0.30	−0.27	0.27	−0.23											
LBF	0.21	0.79	0.76	−0.14	0.09	0.08										
LF	−0.10	0.77	0.76	0.05	0.24	−0.16	0.82									
LHF	0.22	0.002	0.03	0.47	−0.40	0.51	0.25	0.19								
LChl	−0.21	0.38	0.33	−0.02	0.21	0.21	0.08	0.09	0.16							
SP	−0.23	−0.36	−0.34	0.22	−0.23	0.48	−0.15	−0.30	0.09	0.04						
SBF	0.35	−0.158	−0.13	0.39	−0.16	0.04	0.05	0.05	0.41	−0.23	−0.04					
SF	0.71	0.33	0.37	0.37	−0.005	0.003	0.39	0.32	0.21	−0.11	−0.03	0.71				
SPr	−0.25	−0.39	−0.36	0.26	−0.26	0.65	−0.11	−0.30	0.20	0.09	0.98	−0.03	−0.03			
SHF	−0.09	0.09	0.11	−0.20	0.76	−0.46	−0.04	0.07	−0.48	−0.20	−0.40	−0.20	−0.28	−0.45		
SZea	0.03	−0.35	−0.33	0.21	−0.42	0.866	−0.02	−0.34	0.41	0.23	0.62	−0.01	0.10	0.73	−0.58	
SChl b	−0.21	−0.33	−0.34	0.30	−0.43	0.42	−0.07	−0.08	0.38	0.47	0.37	0.08	0.19	0.41	−0.62	0.57

The significance of the correlation is based on the p value (p > 0.05) obtained for a 95% confidence interval (data not shown). Values in red are significantly negatively correlated in and values in yellow are significantly positively correlated. The correlation between macronutrients and the pigments representative of the different phytoplankton species found in the community were analyzed. Pigments associated with the large (L, > 10μm) and the small (S, 0.8–10μm) phytoplankton communities were distinguished. The parameters selected are silicic acid (SI), $NO_2 + NO_3$ (NOx); phosphates (Ph); ammonia (A); nitrite (N); Chlorophyll b (Chl b); Peridin (P); 19-But-Fucoxanthin (BF); Fucoxanthin (F); 19-Hex-fucoxanthin (HF); Prasinoxanthin (Pr); zeaxanthin (Zea).

Table A5 | Pearson correlation table showing the coefficient of correlation between two parameters considering all stations and al depths (0–125 m).

Variables	Co	Ni	Cu	Zn	Cd	Fe	Zn/Co	LP	LBF	LF	LHF	LChl b	SP	SBF	SF	SPr	SHF	SZea
Ni	0.90																	
Cu	0.77	0.91																
Zn	0.72	0.63	0.51															
Cd	0.90	0.93	0.82	0.75														
Fe	−0.55	−0.54	−0.40	−0.77	−0.55													
Zn/Co	0.13	0.14	0.08	0.71	0.23	−0.74												
LP	−0.30	−0.23	−0.24	−0.34	−0.22	0.52	−0.24											
LBF	0.54	0.77	0.66	0.15	0.62	−0.19	−0.28	0.08										
LF	0.65	0.73	0.58	0.33	0.64	−0.40	−0.18	−0.16	0.82									
LHF	−0.15	−0.09	0.08	−0.50	−0.17	0.47	−0.67	0.51	0.25	020								
LChl b	−0.08	−0.11	−0.15	−0.05	−0.22	0.06	−0.04	0.21	0.08	0.09	0.16							
SP	−0.47	−0.27	−0.28	−0.33	−0.30	0.11	0.30	0.48	−0.15	−0.30	0.09	0.04						
SBF	0.18	0.02	0.04	−0.20	0.07	0.18	−0.37	0.04	0.05	0.05	0.41	−0.23	−0.04					
SF	0.34	0.33	0.13	0.16	0.34	−0.24	−0.02	0.003	0.39	0.32	0.21	−0.11	−0.03	0.71				
SPr	−0.47	−0.28	−0.30	−0.37	−0.32	0.22	0.21	0.65	−0.11	−0.30	0.20	0.09	0.98	−0.03	−0.03			
SHF	0.26	0.25	0.35	0.64	0.27	0.42	0.43	0.460	−0.04	0.07	−0.48	−0.20	−0.40	−0.20	−0.28	−0.45		
SZea	−0.55	−0.37	−0.38	−0.54	−0.40	0.55	−0.20	0.86	−0.02	−0.34	0.41	0.23	0.62	−0.01	0.10	0.73	−0.58	
SChl b	−0.48	−0.49	−0.58	−0.36	−0.49	0.21	−0.03	0.42	−0.07	−0.08	0.38	0.47	0.37	0.08	0.20	0.41	−0.62	0.57

The significance of the correlation is based on the p value (p > 0.05) obtained for a 95% confidence interval (data not shown). Values in red are significantly negatively correlated in and values in yellow are significantly positively correlated. The correlation between micronutrients and the pigments representative of the different phytoplankton species found in the community were analyzed. Pigments associated with the large (L, > 10μ.m) and the small (S, 0.8–10μ.m) phytoplankton communities were distinguished. The parameters selected are cobalt (Co); nickel (Ni); copper (Cu); zinc (Zn); cadmium (Cd); iron (Fe); sum of Chlorophyll c (Chl c sum); Chlorophyll b (Chl b); Peridin (P); 19- But-Fucoxanthin (BF); Fucoxanthin (F); 19-Hex-fucoxanthin (HF); Prasinoxanthin (Pr); zeaxanthin (Zea). Fe data are from Lannuzel et al. (2011).

FIGURE A1 | Disappearance ratio of dissolved micronutrients Co (A), Zn (B), Cd (C), Ni (D), Cu (E), Fe (F) and macronutrient (NO$_x$, G) with dissolved phosphate (PO$_4$) for the top 100 m for the Subantarctic and Polar Frontal Zone (Australian sector). Depths and stations are distinguished by different symbol. The slope and the coefficient of correlation for linear regression are shown. Data from a previous study in the region is also shown (Ellwood, 2008). It is to be noted that Ellwood (2008) did not cross the North Polar Front into Antarctic Zone, which could explain some discrepancy. Data for Fe are from Lannuzel et al. (2011).

FIGURE A2 | Disappearance ratio of dissolved micronutrients (Zn, Co, Cd, Fe) with dissolved NO$_x$ (NO$_2$ + NO$_3$, panels, A, B, C, D, respectively) and silicic acid (Si, panels E, F, G, H, respectively) for the top 100 m for the Subantarctic and Polar Frontal Zone (Australian sector). Depths and stations are not differentiated. The slope and the coefficient of correlation for linear regression are shown. Data from a previous study in the region is also shown (Ellwood, 2008). It is to be noted that Ellwood (2008) did not cross the North Polar Front into Antarctic Zone, which could explain some discrepancy. Data for Fe are from Lannuzel et al. (2011).